


## RESEARCH ARTICLE

WILEY

# UAV LiDAR in coastal environments: Archaeological case studies from Tierra del Fuego, Argentina, and Vega, Norway

Ole Risbøl<sup>1</sup>  | Jo Sindre P. Eidshaug<sup>1</sup> | Hein B. Bjerck<sup>1</sup> | Magnar M. Gran<sup>1</sup> | Kristoffer R. Rantala<sup>1</sup> | Angélica M. Tivoli<sup>2</sup> | Atilio Francisco J. Zangrando<sup>2</sup>

<sup>1</sup>Department of Archaeology and Cultural History, NTNU University Museum, Trondheim, Norway

<sup>2</sup>CADIC-CONICET (Centro Austral de Investigaciones Científicas del Consejo Nacional de Investigaciones Científicas y Técnicas), Ushuaia, Tierra del Fuego, Argentina

**Correspondence**

Ole Risbøl, Department of Archaeology and Cultural History, NTNU University Museum, 7012 Trondheim, Norway.  
Email: [ole.risbol@ntnu.no](mailto:ole.risbol@ntnu.no)

**Funding information**

Research Council of Norway; Centro Austral de Investigaciones Científicas/Consejo Nacional de Investigaciones Científicas y Técnicas (CADIC-CONICET); Department of Archaeology and Cultural History at the Norwegian University of Science and Technology (NTNU) University Museum; Agencia Nacional de Promoción de la Investigación, el Desarrollo Tecnológico y la Innovación

**Abstract**

LiDAR has become fairly integrated into archaeological practice at a global scale. This has gradually evolved to include UAV LiDAR. Nevertheless, considerable biases remain, including with regard to geographical regions, chronological periods, feature types and environments. At present, few studies of coastal environments exist, despite the fact that LiDAR—and UAV LiDAR in particular—has the obvious advantages of flexibility and time efficiency in such archaeologically rich but logistically challenging environments. In this paper, we compare the results of UAV LiDAR surveys with records from previous ground surveys in two case studies from coastal environments on opposite sides of the globe. Case Study I of shell middens located within approximately 3 km<sup>2</sup> around Cambaceres Bay involved the first collection of LiDAR data from Tierra del Fuego, Argentina. Case Study II covered approximately 3 km<sup>2</sup> of the island of Vega, Northern Norway, and is among the pioneering LiDAR studies of Mesolithic house pits. The detection success rate was fairly good for Cambaceres—69% of 1240 recorded structures were identified on LiDAR—and above expected for Vega, with 81% of 51 recorded house pits identified on LiDAR. In Cambaceres, the main challenges were dense and low vegetation and identifying small middens. Possible new identifications of archaeological features were made in both areas: subtle depressions interpreted as dwelling foundations in Cambaceres and house pits on Vega. We conclude that UAV LiDAR can contribute to coastal archaeology and that it has added values besides making new identifications, being both flexible and time efficient. An example pertains to the possible identification of a practice that has not previously been proved archaeologically in Tierra del Fuego—more thorough site preparation prior to the construction of the dwellings—which in turn raises new questions.

**KEYWORDS**

airborne laser scanning, dwellings, house pits, Mesolithic, shell middens, shell rings and mounds

This is an open access article under the terms of the [Creative Commons Attribution](https://creativecommons.org/licenses/by/4.0/) License, which permits use, distribution and reproduction in any medium, provided the original work is properly cited.

© 2023 The Authors. *Archaeological Prospection* published by John Wiley & Sons Ltd.

## 1 | INTRODUCTION

This paper is linked to the Norwegian–Argentine research collaboration Marine Ventures, which studies the variety of human–sea relations based on evidence related to settlement structures, subsistence, ethnography and mobility risk assessments among marine foragers from high-latitude seascapes (Bjerck, Breivik, et al., 2016; Bjerck & Zangrando, 2013). From a comparative perspective, which includes insights from different academic traditions, this collaboration has focused on two coastal areas located on opposite sides of the globe: the Beagle Channel in Tierra del Fuego, Argentina, and the island of Vega in Northern Norway (Figure 1). In 2022, UAV (*unmanned aerial vehicle*) LiDAR campaigns were conducted under the auspices of the Marine Ventures project in both areas.

LiDAR became commercially available as a way of mapping landscapes in the late 1990s. Since being introduced to archaeology just after the millennium, its use for archaeological purposes has increased persistently across large parts of the globe. Nonetheless, there are regions where LiDAR still has not been applied due to reasons such as expenses, challenging logistics, lack of training or possibilities to utilize spatial techniques. Tierra del Fuego represented such an example before this project. The application of LiDAR in archaeology is further biased in terms of *chronology* and *types of features*. In Europe, most LiDAR projects focus on cultural monuments, features and sites from the Iron Age and the Middle Ages. In recent years, the focus area has

widened to include LiDAR-based studies of Neolithic and Bronze Age sites and monuments (e.g., Guyot et al., 2018; Mihiu-Pintilie et al., 2022; Sánchez Díaz et al., 2022; Żurkiewicz, 2022). The use of LiDAR to examine Mesolithic settlement structures, like in this study, is still very rare. The reason may be that one simply does not expect LiDAR to be the right method for identifying and mapping such features. Finally, what kinds of *environments* LiDAR is applied to is also biased. For instance, applications in coastal environments like those of the Beagle Channel and Vega are less common even though the situation has improved, for example, due to employment of airborne laser bathymetry in combination with LiDAR (Doneus et al., 2013, 2020).

The Beagle Channel and the southernmost Pacific archipelagos in South America were inhabited by marine foragers for more than 7000 years. The Fuegians were mobile hunter-fisher-gatherers who travelled by sea and lived in branch huts close to the water, developing a marine subsistence strategy based on marine mammals, fish, sea birds and shellfish (Lothrop, 1928). As refuse accumulated at their settlements, marked shell middens of various shapes and sizes were formed, resulting from repeated occupations at the same place at scales of centuries or millennia (Orquera & Piana, 1989–1990; Piana & Orquera, 2010; Zangrando, 2018). A typical cultural practice in the Beagle Channel was to deposit refuse around the huts, where the accumulation of shells and other debris through reoccupations over a long time created sheltering structures. Clusters of such ring-shaped dwelling remains (some of them counting more than 100) are found along the



**FIGURE 1** Map showing the location of the two study areas in their respective hemispheres. The photos illustrate how the coastal landscape typically appears in these areas. Illustration: Magnar M. Gran. [Colour figure can be viewed at [wileyonlinelibrary.com](https://onlinelibrary.wiley.com/terms-and-conditions)]



coastline (Figure 2), usually close to the shore. The Fuegian marine foragers and their descendants, the Yagan (Figure 3), have been studied through detailed archaeological excavations and surveys, as well as written and photographic sources (e.g., Butto et al., 2018; Fiore et al., 2014, 2021; Orquera et al., 2011; Orquera & Piana, 1999, 2009, 2015;

Zangrando, 2018). However, with a few exceptions (Barceló et al., 2002; Bjerck, Zangrando, et al., 2016), studies about settlement patterns at a larger landscape scale remain scarce in the region.

In sharp contrast to the prominent shell middens of Tierra del Fuego, the 'archaeological visibility' of the earliest marine foragers in



**FIGURE 2** A cluster of ring-shaped shell middens at Binushmuka, Cambaceres Bay. Photo: Ole Risbøl. [Colour figure can be viewed at [wileyonlinelibrary.com](https://onlinelibrary.wiley.com/doi/10.1002/arj.1918)]

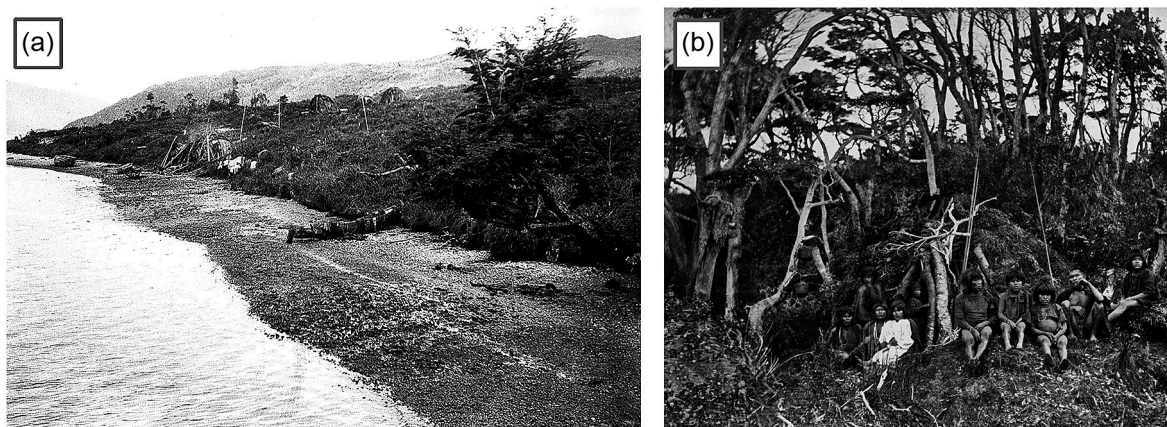


**FIGURE 3** Yagan dwellings. (a) Yagan settlement close to the shore. Photographer: Unknown. (b) A Yagan family resting at the ring-shaped shell midden around their dwelling hut. Photo: Doze and Payen (1882–1883).





**FIGURE 4** House pits at Vega. (a) Trond Tøgersen is standing on the wall formation of the house pit at the hunting station Porsmyrdalen 3. (b) One of the 19 house pit house foundations at the residential camp Åsgarden during excavation in 1987. The house is 14C-dated to 9400 BP. The main difference between the two sites is the artefact composition: Hunting stations display higher tool ratios and considerably lower amounts of lithic waste. Photos: Hein B. Bjerck. [Colour figure can be viewed at [wileyonlinelibrary.com](https://onlinelibrary.wiley.com/doi/10.1002/arj.1918)]

Norway mostly arises from lithic scatters in subsoil sediments. During the Mesolithic (c. 11 500–6000 BP), they gradually developed a more sedentary lifestyle as is recognizable in more substantial cultural deposits, changes in the lithic distribution pattern and the appearance of pit houses—the earliest known permanent dwelling structures in Norway—around 9500 BP<sup>1</sup> (Bjerck, 1990, 2008) (Figure 4). Mesolithic sites are typically shore-bound and due to a post-glacial rebound, they are usually situated considerably higher than the present shoreline. This also means that the landscape looked dramatically different in the past compared with its present appearance, although it has retained its archipelagic character. The Mesolithic has been examined thoroughly based on archaeological and environmental data, with emphasis on settlement patterns and dwellings in coastal areas (e.g., Bjerck, 2007, 2008; Breivik, 2016; Fretheim, 2017; Fretheim et al., 2018; Schülke, 2020). However, although the use of LiDAR to study early Holocene sea level changes and reconstruct paleo-landscapes is not uncommon, few studies have applied LiDAR for systematic supra-regional studies of Mesolithic settlement patterns. One exception is Damm et al. (2021), who used LiDAR as one of their methodological approaches in searching for Mesolithic house pits (see also Damm & Skandfer, 2021).

The aim of this paper is to examine how LiDAR from drones (UAV LiDAR) can contribute to coastal landscape archaeology. Such studies presuppose knowledge about archaeological features at a large spatial

scale. However, coasts and islands that were favoured in the past can often be quite inaccessible today. This is true of the archipelagic coasts in Norway and Tierra del Fuego, where past shorelines tended to be displaced landward after the first pioneers arrived. In this paper, we apply case studies from the north coast of the Beagle Channel and the island of Vega to compare the detection success of UAV LiDAR with conventional pedestrian field surveys. Our objectives are to

1. quantify and compare the detection success rates of UAV LiDAR and conventional field survey data in the case study areas and
2. determine and discuss the causes of the detection success rates for the different categories of archaeological features identified with UAV LiDAR in the case study areas.

Finally, we briefly discuss the added value of LiDAR to studies of marine lifestyles, coastal landscapes and settlement patterns.

## 2 | BACKGROUND

The implementation of remote sensing is of special importance in regions with extensive littoral areas. Coasts are highly productive environments, and consequently, the long-term human use has resulted in the presence of many archaeological features along the coastlines. However, long distances and rough seas might hamper fieldwork in such areas, making archaeological survey logistics a huge

<sup>1</sup>All radiocarbon dates are calibrated to calendar years.



challenge, being both risky and time-consuming. Remote sensing methods, like LiDAR, can ease fieldwork and be used effectively to collect detailed information about archaeological surface features at a landscape scale.

The Beagle Channel is extraordinarily apt for remote sensing and three-dimensional (3D) modelling. Shell middens here are remarkably visible and there are few modern disturbances in the area. In addition, the landscape along the Beagle Channel is poorly mapped with only coarse maps existing (Barceló et al., 2002). Although Google Earth has proved to be a great tool for planning and conducting fieldwork in the region, it has obvious limitations for detailed landscape studies. The resolution of the satellite imagery used in Google Earth varies considerably across the globe, and although it has improved in recent years, it remains rather low in many places in Tierra del Fuego. Furthermore, given that Google Earth is a passive remote sensing method based on satellite photographic images, visual access to the ground below dense vegetation is nearly impossible (Casana et al., 2021). On the other hand, an active method like LiDAR, with its ability to penetrate vegetation, enables one to filter away vegetation and generate very detailed high-resolution 3D bare-earth terrain models (Crutchley, 2009). Thus, we employed LiDAR mapping within selected areas along the Beagle Channel based on the reasoning that LiDAR-generated 3D digital terrain models (DTMs) would bring about an excellent basis for studies at a larger spatial scale than what has previously been possible.

Vega is rather well mapped as both cadastral maps (1:5000) and aerial orthophotos are available. The island was also airborne laser scanned as part of the Norwegian national LiDAR mapping campaign conducted from 2016 to 2022. The national coverage was carried out with two points per square metre as standard resolution.<sup>2</sup> Even though the data from the national campaign are useable for archaeological purposes to some extent, they are not optimal. A previous study has shown that at least five points per square metre are preferred for mapping archaeology (Bollandsås et al., 2012), while another study has suggested eight points per square metre as ideal (Optiz, 2016). With the same justification as for Tierra del Fuego, we wanted to test out a high-resolution UAV LiDAR mapping of Mesolithic settlement structures on Vega.

## 2.1 | UAV LiDAR

Technological developments in recent years have led to a situation where UAV-based LiDAR mapping has become a viable alternative for acquiring high-resolution 3D data. UAV LiDAR fills a gap between more remote airborne laser scanning (ALS) from a plane or a helicopter on the one hand and terrestrial laser scanning from the ground on the other (Adamopoulos & Rinaudo, 2020). The latter methods have been used within archaeology for more than two decades; in particular, ALS has been established as a preferential way of mapping sites

and landscapes by archaeologists engaged with remote sensing. The opportunity of deploying UAV LiDAR for archaeological purposes is quite new, having been first mentioned as a potential application in 2017 (Campana, 2017). It was immediately followed by published studies in which UAV LiDAR was used to identify cultural features and monuments in wooded environments in various parts of the world (Khan et al., 2017; Murtha et al., 2019; Risbøl & Gustavsen, 2018).

The most important advantages of UAV LiDAR are its flexibility in terms of use and the possibility it provides of mapping areas with very high point densities and thus generating DTMs with very high resolution, enabled by low flight altitude and low flight speed. On the other hand, limited flight time due to restricted battery capacity and vulnerability in terms of weather conditions (especially strong winds) represent disadvantages, together with cost issues. Even though prices are decreasing, it is still economically demanding to purchase the equipment: The sensor is particularly expensive.

Although the use of UAV LiDAR in archaeology remains limited compared with conventional LiDAR, it has been successfully employed to detect archaeological features under tree canopies in various environments across the world. This includes building foundations and field systems in Hawaii (Casana et al., 2021; McCoy et al., 2022), building features from a deserted village in Italy (Masini et al., 2022), deserted settlements in Spain (Monterroso-Checa et al., 2021), grave mounds and charcoal production sites in Norway (Risbøl & Gustavsen, 2018), graves and clearance cairns in Finland (Roiha et al., 2021), building features and field systems in Mexico (Schroder et al., 2021), mapping historical conflict landscapes in Germany (Storch et al., 2022), an ancient walled settlement in Peru (VanValkenburgh et al., 2020) and mounds and building foundations in China (Zhou et al., 2020). Most of these projects involved field verifications of LiDAR identifications or evaluations of previous field surveys by employing LiDAR mapping.

A few projects in which LiDAR was used to investigate shell middens are particularly relevant for our study. Barbour et al. (2019) used UAV LiDAR to map shell-ring architecture on the Gulf Coast of Florida. Conventional LiDAR has been employed to study the spatial distribution of shell rings in coastal South Carolina (Davis et al., 2019) and shell-ring building practices throughout the Southeastern United States (Davis et al., 2020, 2021; Randall, 2014). Emmitt et al. (2020) recently mapped and studied shell mounds situated at Cape York Peninsula in Australia. However, as mentioned above, prior to the project presented in this paper, neither UAV nor conventional LiDAR had been used as a methodological approach in archaeology in Tierra del Fuego.

## 2.2 | Case Study I: Cambaceres Bay (Argentina)

Cambaceres Bay is located on the northern shores of the Beagle Channel in Argentinean Tierra del Fuego (Figure 5). The area is situated within a drumlin field, which creates a favourable topographic situation, with many sheltered and semi-enclosed bays scattered among

<sup>2</sup>This is the commissioned resolution, but as usual, the actual distribution of ground points varies throughout the landscape.



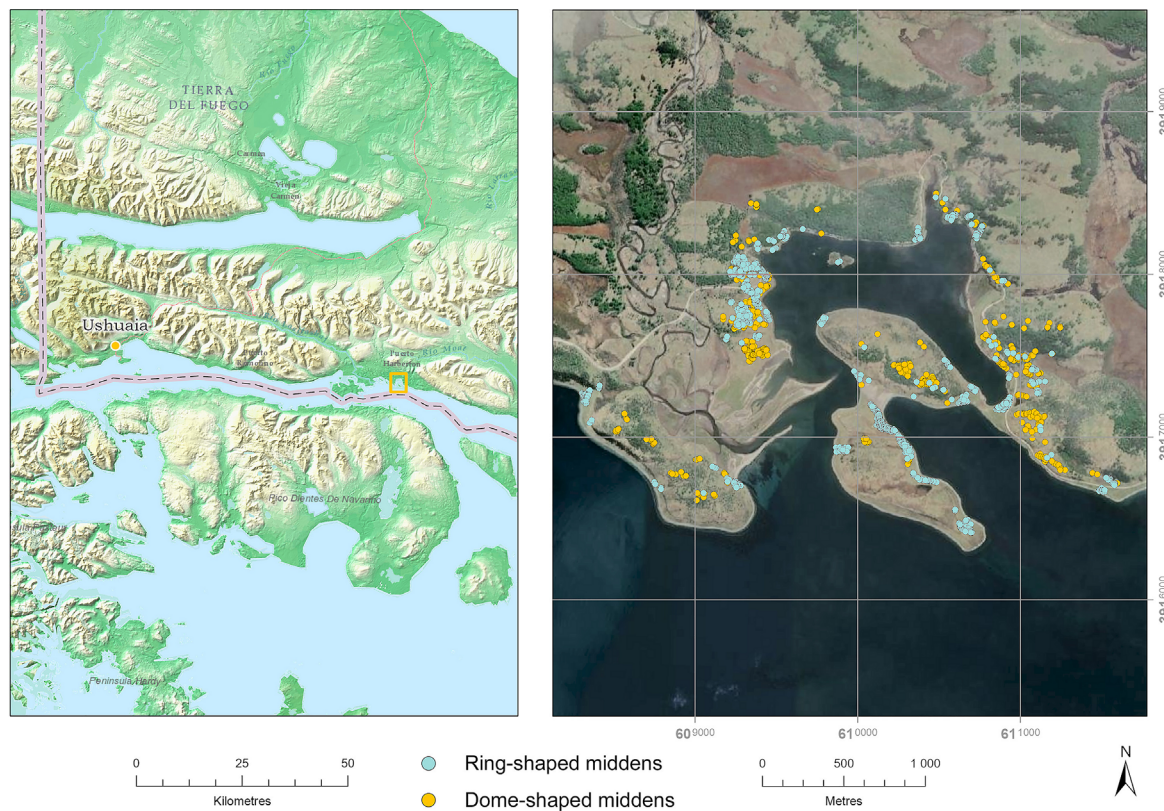


**FIGURE 5** The shell midden features mapped during the Cambaceres Surveys on the northern coast of the Beagle Channel (based on Bjerck, Zangrando, et al., 2016). Illustration: Magnar M. Gran. [Colour figure can be viewed at [wileyonlinelibrary.com](https://onlinelibrary.wiley.com/doi/10.1002/arj.1918)]

the drumlin hills and peninsulas. The areas closest to the shore are generally more sparsely covered by trees than those farther away, including the drumlin ridges. The oldest raised beaches in the bay date to about 6700 BP, and in Cambaceres, they are located about 5.5 m above sea level (a.s.l.) (Zangrando et al., 2016).

The Cambaceres Surveys were carried out between 2009 and 2013 and included a systematic terrestrial survey of shell midden structures in the Cambaceres Bay area, which was mostly based on surface observations. It recorded 1251 structures across an area of about 3.5 km<sup>2</sup> (Figure 5). The archaeological structures span from c. 7500 BP to recent times (Bjerck, Zangrando, et al., 2016).

Although different types of shell middens can be identified in the Beagle Channel based on their surface morphologies (Orquera & Piana, 1989–1990), two specific categories are mainly recorded in the archaeological landscape (Barceló et al., 2002): *ring-* and *dome-shaped structures*. Later, Bjerck, Zangrando, et al. (2016) named them dwelling pits (or dwelling structures) and shell midden domes, respectively. For the sake of simplicity, we adopt the traditional terminology of ring- and dome-shaped middens in this paper. However, we underscore that the crucial difference between them pertains to whether the shell midden can be linked to an adjacent dwelling structure through visible traces on the surface, even though both categories may be associated with dwelling sites (see below). These visible traces occur as circular depressions that typically have a diameter of 3–4 m (Piana & Orquera, 2010), which are most perceptible in the distinct ring-shaped

shell middens (Figures 3 and 6). According to archaeological and ethnographic information (Orquera & Piana, 1989–1990), these structures result from a deposition practice that creates a footprint of the dwelling structure (the foundation) in the shape of a depression in the middle of the midden mound. If not ring-shaped, the midden adjacent to the former dwelling structure may also be a semi-enclosed ring, crescent-shaped or even dome-shaped. Thus, we use ring-shaped middens as a collective term for the identification of all types of middens adjacent to dwelling structures. To clarify: in this paper, the term *ring-shaped middens* is synonymous with and hereafter replaces the terms *dwelling pit* and *dwelling structure*, as used in the Cambaceres Surveys report (Bjerck, Zangrando, et al., 2016). In the survey, the *ring-shaped middens* were further subdivided into *large ring-shaped middens*, associated with midden walls higher than about 0.4 m, and *small ring-shaped middens*, associated with midden walls lower than about 0.4 m.

We employ the synonymous terms *dome* and *dome-shaped midden* exactly as in the report (Bjerck, Zangrando, et al., 2016), reserving these for isolated shell midden structures that have *no visible traces* from an *adjacent dwelling structure*. Although archaeological excavations have proved that dwelling spaces can also be located next to domes (Zangrando et al., 2014), multiple activities have been recorded in association with dome sites (e.g., Álvarez et al., 2013; Piana & Canale, 1993–1994; Zangrando et al., 2014). As the name indicates, *domes* are shell middens that usually have the shape of a mound





**FIGURE 6** A ring-shaped shell midden in Harberton, arranged around a former dwelling. Lime-loving white clovers indicate buried shell refuse. Photo: Hein B. Bjerck. [Colour figure can be viewed at [wileyonlinelibrary.com](http://wileyonlinelibrary.com)]

(Figure 7), although some of them can be very small and contain merely a thin layer of midden material (Bjerck, Zangrando, et al., 2016, p. 33). The *dome-shaped middens* were subdivided into four categories according to volume estimates: *very large domes* ( $>5.2 \text{ m}^3$ ), *large domes* ( $2.6\text{--}5.2 \text{ m}^3$ ), *medium domes* ( $0.5\text{--}2.6 \text{ m}^3$ ) and *small domes* ( $<0.5 \text{ m}^3$ ).<sup>3</sup>

Among the archaeological structures that were recorded during the Cambaceres Surveys, 804 structures were interpreted as ring-shaped middens, while 432 were interpreted as domes. The other two types of visible structures were *Casa Grande*, an extremely large shell midden with a diameter of 15 m and walls with a stratigraphic sequence of more than 1.5 m (Bjerck et al., 2019), and three possible canoe runways. The latter most likely relate to the chiefly post-1880 heavier dugout canoe as opposed to the traditional bark canoe. All in all, the Cambaceres Surveys permitted a comprehensive understanding of settlement structures and the locations of settlements in the landscape.

### 2.3 | Case Study II: Vega (Norway)

Vega is an island and archipelago situated some 15 km off the Nordland County mainland in Northern Norway, about 100 km south of the Arctic Circle (Figure 8). The main island is dominated by its western-facing mountain, peaking at 800 m a.s.l., while most of the lowlands behind the island's rocky coastline with its many sheltered bays consist of cultivated land interspersed among exposed abraded

bedrock ridges. Due to the post-glacial rebound and the considerable shoreline displacement on Vega, the earliest shore-bound archaeological sites (c. 10 000 BP) are located on raised beaches at about 80 m a.s.l. (Bjerck, 1990), just below the marine limit at 96 m a.s.l. At that time, the main island of the archipelago was much smaller. Apart from the planted spruce in parts of the island, tall vegetation is quite sparse in the rough coastal environment on Vega.

Vega was partly surveyed in 1985–1987 within the approximated elevation intervals 60–70, 50–60 and 25–35 m, whose raised shorelines at the interval minimums date to c. 8–9000, c. 7–8000 and c. 4–5000 BP, respectively (Bjerck, 1989). The survey had a strategic focus on the relationship between settlement location and landscape, and factors such as sheltered harbours came to play a significant role in succeeding studies. Test-pitting was the preferred field method, as most lithic remains from the Mesolithic are found in subsoil deposits between bedrock ridges. However, during the surveys, a total of 45 house pits visible above ground were recorded within the areas covered by this case study, a number that subsequently has increased to 51 (Figure 8). Eleven of these are uncertain because they have not been verified in the field. House pits are often visible on the surface as rather shallow rounded depressions enclosed or semi-enclosed by a low wall mound (Figure 4). They are quite uniform in size, typically measuring 3–4 m in diameter (Bjerck, 1989).

## 3 | METHODS

Five areas of approximately  $15 \text{ km}^2$  in total were scanned on the Beagle Channel coast, while four areas of about  $4 \text{ km}^2$  in total were

<sup>3</sup>Volumes of deposits above the surface, calculated from a semi-ellipsoid formula based on field estimates of length, width and height. Note that the report applies the prism formula as a simplification, because it does not affect relative figures (Bjerck, Zangrando, et al., 2016, p. 28). The difference between prism and semi-ellipsoid is a constant of  $\sim 0.524$ .





**FIGURE 7** Examples of dome-shaped middens from the Beagle Channel. (a) A very large dome on the right side situated in an area with several smaller domes, which are hard to spot in among the low bushes and high grass growing on the drumlin ridge, Central Peninsula, Cambaceras. Photo: Jo Sindre P. Eidshaug. (b) Profile view from excavation of Heshkaia 35 at Moat, east of Cambaceras. Photo: Atilio Francisco J. Zangrando. [Colour figure can be viewed at [wileyonlinelibrary.com](https://onlinelibrary.wiley.com/terms-and-conditions)]

scanned on Vega. For this paper, we have selected two areas of about 3 km<sup>2</sup>: one with two bays in Cambaceras in the Beagle Channel (Figure 9) and another on Vega that encompassed the three locations Åsgarden–Porsmyrdalen, Floaskaret–Skavdalen and Middagskarheia–Hammaren (Figure 10). Given that the ground survey at Vega was confined to mentioned elevation intervals, it only encompassed about 1 km<sup>2</sup> within the areas covered by the UAV survey. Nevertheless, we decided to include the entire UAV-surveyed area in the study because some of the known house pits were located outside the elevation intervals. However, the discrepancies in survey intensity were respected when we compared the two areas (as reflected in Sections 4 and 5).

### 3.1 | Data collection and processing

We collected the LiDAR data with a Riegl miniVUX-3 UAV LiDAR sensor mounted on a DJI Matrice 600 Pro drone (hexacopter) (Figure 11).

Flight data were recorded with an onboard Applanix APX-20 UAV GNSS/IMU unit and combined with a Carlton BRx7 base station. GNSS corrections from base station data were added in post-processing, using Applanix POSPac software. Control points were not used. This allowed us to generate high-resolution DTMs with substantially higher point densities compared with conventional airborne LiDAR. Furthermore, UAV LiDAR provided advantageous logistical flexibility in rugged coastal landscapes like the ones studied here.

Table 1 displays the metadata from Cambaceras and Vega. As both weather (wind and rain) and logistics were likely to affect flight time, we applied settings that would maximize area coverage without significant data loss in Cambaceras. Hence, flight altitude and speed were higher than on Vega, while the (boustrophedon) line pattern was prioritized over the double grid pattern in both survey areas for increased coverage.

Both campaigns were carried out during autumn in the respective hemispheres but with different situations regarding vegetation. In



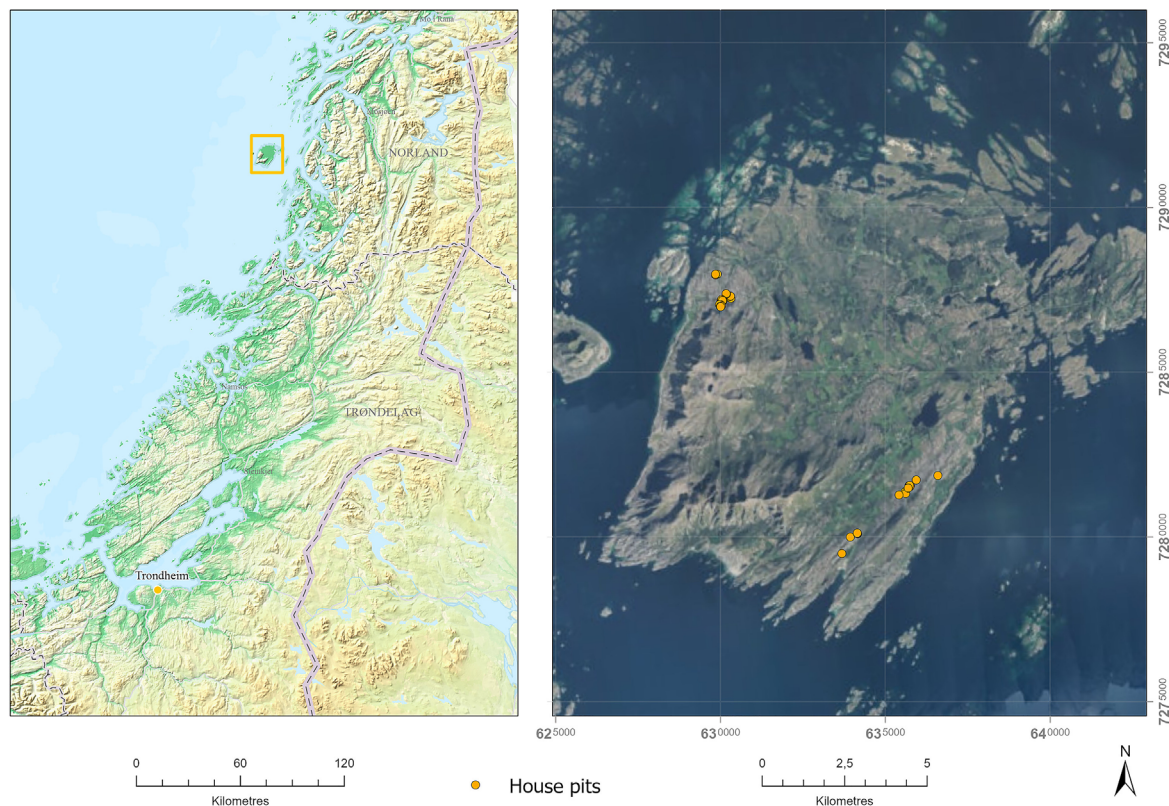


**FIGURE 8** The house pits located within the case study areas on Vega. Illustration: Magnar M. Gran. [Colour figure can be viewed at [wileyonlinelibrary.com](https://onlinelibrary.wiley.com/doi/10.1002/arj.1918)]

Tierra del Fuego, where the predominant species is *Nothofagus*, of which *N. pumilio* is deciduous and *N. betuloides* is evergreen, the scanning was carried out before proper defoliation. On Vega, the deciduous trees (mostly *Betula*) had lost almost all their leaves by the time the scanning took place. Nonetheless, there were challenges in terms of planted conifers on Vega.

The LiDAR raw data were processed in POSPac (Applanix) and RiPROCESS (Riegl). Riegl filtering algorithms were used to classify point clouds into vegetation points and ground points, enabling us to create DTMs devoid of vegetation as a well-suited basis for our interpretations. Classified point clouds were exported in LAS format (Version 1.4) and used for generating DTMs with a raster resolution of 0.1 m in ArcGIS.

Relief visualization techniques were applied to enhance the visibility of the archaeological feature types that were known from the case study areas (Figures 12 and 13). Such techniques are developed to increase the visibility of subtle convex and concave features. Local relief models (LRMs) based on Hesse (2010), as well as slope and analytical hill-shading models, were created from the DTMs using ArcGIS. We used the Relief Visualization Toolbox (RVT) Version 2.2.1 (Kokalj & Somrak, 2019; Zakšek et al., 2011) to generate models based on sky-view factor (SVF), negative openness and local dominance (LD). LRMs are highly biased towards small-scale features, while retaining more information about relative elevation compared with simpler difference models (Hesse, 2010). Visualization methods based

on diffuse relief illumination estimated from the proportion of visible sky (SVF) or the mean horizon elevation angle (negative openness) provide detailed information about the relief and are highly useful for detecting small-scale features (Yokoyama et al., 2002; Zakšek et al., 2011). LD shows the degree of dominance of each pixel upon its immediate surroundings and is most apt for visualizing subtle convex features (Hesse, 2016).

### 3.2 | Interpretation, field verification and comparative analysis

The resulting raster files served as the basic data for visual interpretations of the DTMs using ArcGIS, often displayed as blends and supplied by 3D analysis in the LiDAR exploitation software Quick Terrain Modeler (QTM). All anomalies that were interpreted as possible archaeological remains were collected in a database (shapefiles and Excel datasheets). They were ranked in accordance with estimated interpretation confidence ranging from 1 to 4 (1—low, 2—below medium, 3—above medium, 4—high).

To supplement our field-verified data from previous field surveys, a selection of 26 LiDAR-identified anomalies from Cambaceres were subjected to field verification after the interpretation of the LiDAR data. They were checked in the field in 2023 based on visual inspection and test-pitting.



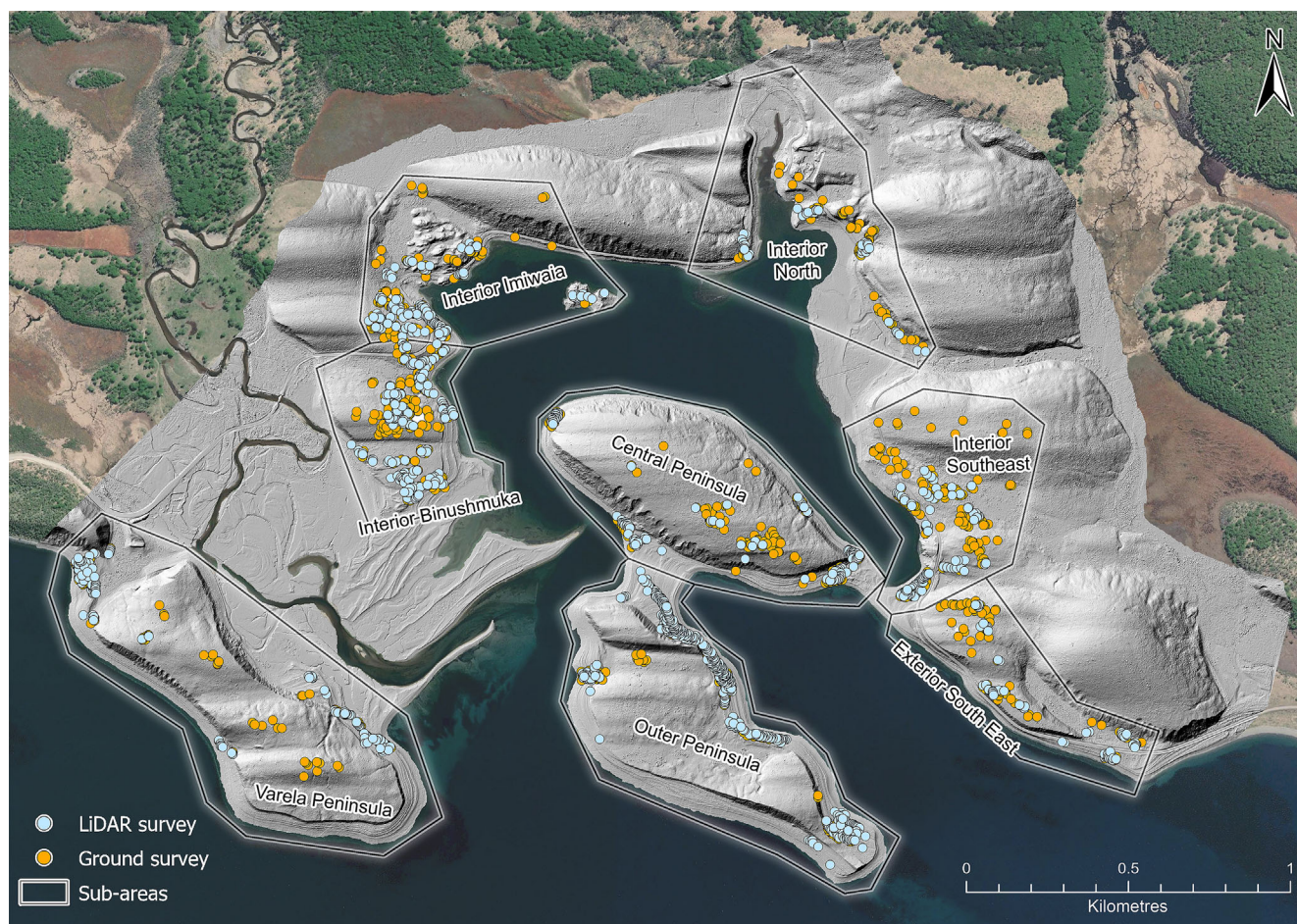


**FIGURE 9** LiDAR survey area in Cambaceres, with LiDAR identifications drawn on top of the features recorded in the previous ground survey within the eight sub-areas included in the case study. Illustration: Magnar M. Gran. [Colour figure can be viewed at [wileyonlinelibrary.com](https://onlinelibrary.wiley.com/doi/10.1002/arj.1918)]

It was not possible to compare the two data sets feature to feature due to the relatively low precision of the positioning from the previous field surveys, which was based on the use of a standard handheld global positioning system (GPS) (Cambaceres) or pre-digital paper maps (Vega). The only exception was 21 house pits on Vega that were mapped with centimetre precision using the CPOS GNSS correction service provided by the Norwegian Mapping Authority. The remaining structures from Vega were georeferenced from field drawings published in Bjerck (1989). For the Cambaceres Survey, the GPS accuracy was reported to vary between  $\pm 3\text{--}5\text{ m}$  in open areas and  $\pm 15\text{--}20\text{ m}$  in wooded areas (Bjerck, Zangrando, et al., 2016, p. 25).

Thus, to compare the data sets, we applied the ArcGIS tool Spatial Join to count feature and feature by type frequencies within clusters based on dissolved buffer polygons with distances set to 20 m from the source (for features with CPOS precision, the distance was set to 2 m). The LiDAR anomalies and the field survey records were used respectively as the sources for two different sets of clusters, thus permitting two-way comparison of matches between the LiDAR and field survey records. Significantly, the comparisons were carried out both with and without respect to feature type (ring- or dome-shaped) in

Cambaceres due to the uncertainties involved in archaeological interpretations. To determine the success rate of the LiDAR and field surveys in terms of feature type and location in Cambaceres, we also compared the 15 largest clusters that were generated from a merge of the two other cluster sets.

We decided that the optimal search radius for possible matches between the two data sets should be 20 m based on a comparison of success rates with 5-, 10- and 20-m search radii within the 15 clusters in Cambaceres (Figure 14). Each cluster was attributed to one category according to vegetational openness (from open to wooded) and one category according to dominant feature type (dome- or ring-shaped). For each category, we summed up the increase in the success rate resulting from extending the search radius by one level. By dividing this sum by the total number of features belonging to that category, we could determine the extent to which openness and feature type were affected by increasing the search radius (Table 5). Although the difference between the 10- and 20-m search radii was marginal, a failure to consider GPS accuracy could result in the false conclusion that a significant number of previously unknown dome-shaped middens in wooded areas only were identified on LiDAR (Figure 14). Although the 20-m search radius yielded a better match between



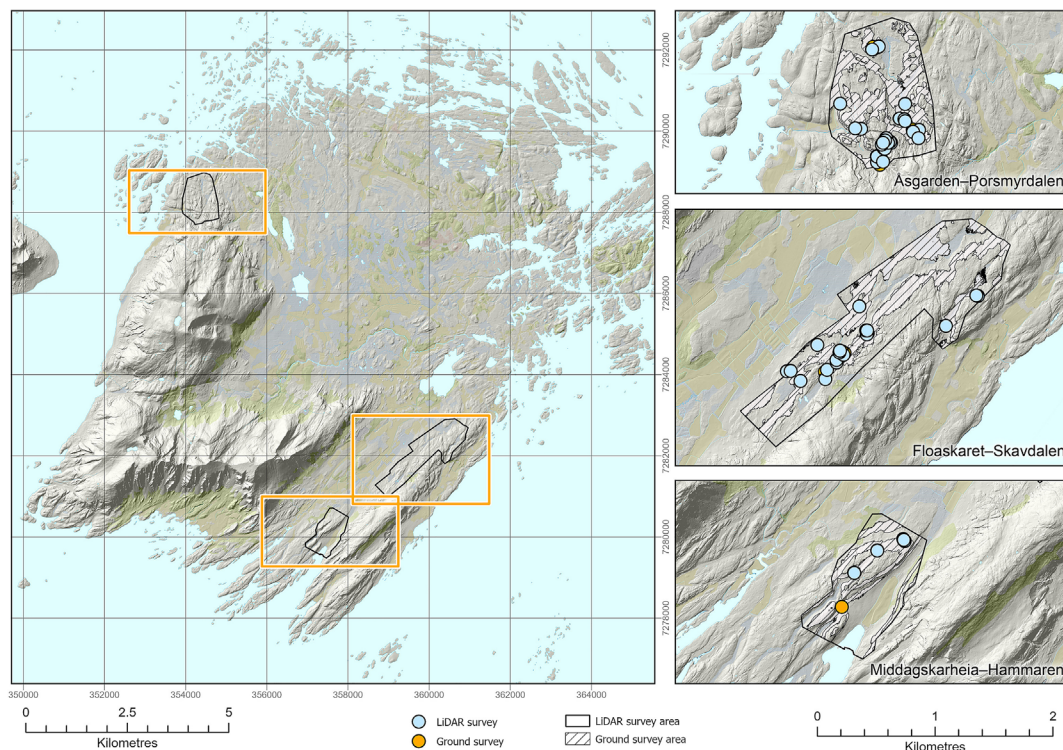


**FIGURE 10** LiDAR survey area included in the case study from Vega, with LiDAR identifications drawn on top of the features recorded in the previous ground survey. Illustration: Magnar M. Gran. [Colour figure can be viewed at [wileyonlinelibrary.com](http://wileyonlinelibrary.com)]

LiDAR and the ground survey, it should be noted that it included some false matches in the count due to diverging distribution patterns between the LiDAR anomalies and the field data. However, compared with possible fallacies embedded in applying a 10-m search radius, the 20-m search radius did not affect the general trend significantly (see Section 4 and Table 5).

## 4 | RESULTS

### 4.1 | Cambaceres

Cambaceres Bay was divided into eight sub-areas during the ground survey (Bjerck, Zangrando, et al., 2016, p. 22) and our area-based LiDAR analysis followed the same sub-division (Figure 9). Within the 3-km<sup>2</sup> study area, a total of 1110 anomalies were identified on the LiDAR-generated models (Table 2), a somewhat smaller number than the 1240 features mapped during the ground survey (Table 3). A total of 253 (23%) of the LiDAR anomalies had no ground survey matches within a 20-m search radius, and vice versa, 382 (31%) of the ground-surveyed features were not among the LiDAR identifications.

As mentioned above, the LiDAR interpretations were divided into four groups based on level of confidence. Fifty-nine per cent of the interpretations fell into the high confidence groups 3 or 4. Thirteen per cent ( $n = 84$ ) of these did not match any of the field-surveyed features. Six of the 26 anomalies identified as ring-shaped middens on LiDAR were verified as such (Table 4). Five of these six anomalies had

been tagged with low confidence (1–2) and the last one as above medium (3). None of the 26 features belonged to the group with high confidence (4). In addition, three anomalies that were classified as likely (3) were among the disproved ones.

The results presented in Table 3 show that the number of LiDAR omissions varied from 14 (6%) on the Outer Peninsula to 86 (49%) in the Interior Southeast, with an average of 48 features in the eight areas. The detection success was substantially higher for ring-shaped than for dome-shaped middens. For the former, the total success rate was 83%, varying from 55% to 99% between the sub-areas. For domes, the total success rate varied from 8% to 59% between the sub-areas, with an average rate of 35%. There was also a clear tendency for large features to be more successfully identified compared with smaller ones. All three possible canoe runways found during the fieldwork were identified on the LiDAR images.

Table 2 shows that 253 of the LiDAR identifications were not among the ones found on the ground survey, which is equivalent to 23%. The bulk of the omissions were ring-shaped middens, adding up to 241 when only matches within the same feature category were counted, while 49 of the LiDAR-identified domes had no match within a 20-m search radius.

The analysis of 15 large clusters of features resulted in 868 field-surveyed features and 817 LiDAR identifications (Figure 15). There were slightly more field-surveyed features compared with LiDAR identifications in nine cases (Clusters 5, 17, 20, 22, 38, 40, 41, 42 and 43). The balance shows 103 more ring-shaped middens among the LiDAR identifications and 154 more dome-shaped middens in the field





**FIGURE 11** We used a Riegl miniVUX-3 UAV LiDAR sensor mounted on a DJI Matrice 600 Pro drone, here in action in Tierra del Fuego. Photo: Ole Risbøl. [Colour figure can be viewed at [wileyonlinelibrary.com](https://onlinelibrary.wiley.com/doi/10.1002/arp.1918)]

**TABLE 1** LiDAR parameters applied in Cambaceres and Vega.

Description	Cambaceres	Vega
Campaign dates	21–30 March 2022	24–26 October 2022
Study area	3 km <sup>2</sup>	3 km <sup>2</sup>
Point spacing	0.10 m	0.08 m
Point density	105 ppm <sup>2</sup>	150 ppm <sup>2</sup>
Ground point density	66 ppm <sup>2</sup>	125 ppm <sup>2</sup>
Flight altitude (above ground level)	107 m	80 m
Flight speed	10 m/s	8 m/s
Side overlap	50%	50%
Scan rate (lines per second)	59.2	56.4
Lat. strip separation	107 m	80 m
Pulse rate	300 kHz	300 kHz

survey record, amounting to 51 more features identified in the field. The matches between the LiDAR and field features were quantified for each cluster in three operations with 5-, 10- and 20-m search radiuses,

respectively (Table 5). In the first case, 307 features did not match (38%), in the second case 176 (22%) and in the third case 158, which is equivalent to 19%. Table 5 also shows that the number of matches increased most in wooded areas and for domes when the search radius was increased. Expanding the search radius from 10 to 20 m had a lower impact on the results than expanding it from 5 to 10 m. The only category that was still quite significantly affected by an increase from 10 to 20 m was the number of matches in wooded areas.

## 4.2 | Vega

Three areas were studied on Vega: Åsgarden–Porsmyrdalen, Floaskaret–Skavdalen and Middagskarheia–Hammaren (Figure 10). The number of field-surveyed house pits was 51, of which 40 were field-verified. Eleven (22%) of the 51 house pits were not identified on the LiDAR-generated models (Table 6). Considering only verified features, the number of LiDAR-identified house pit omissions dropped to five, which is equivalent to 13%. Overall, there was not much variation between the areas in terms of detection success.



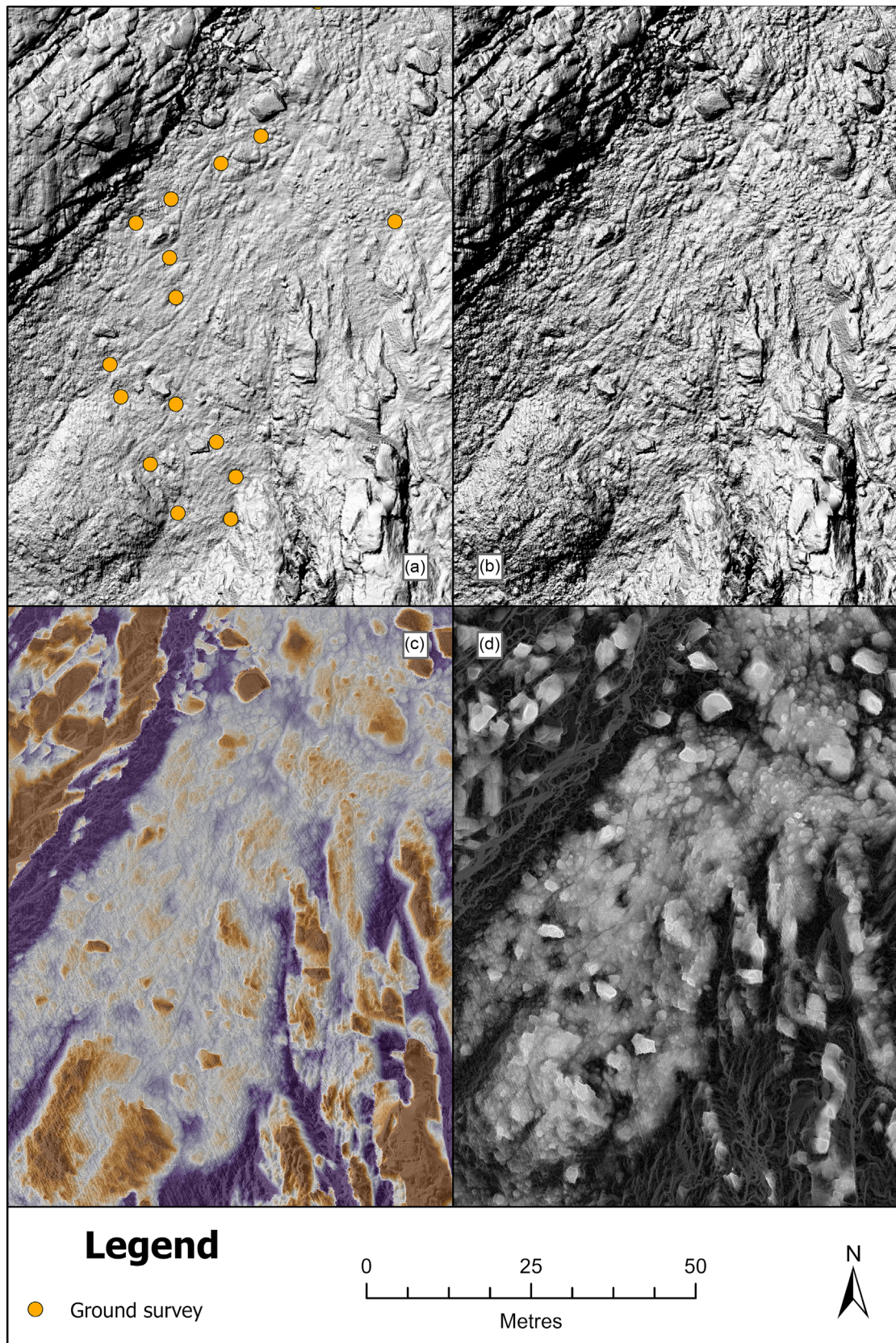


**FIGURE 12** Example I of visualization techniques applied in ArcGIS during the study. (a) Digital elevation model with shaded relief. (b) Hillshade. (c) Local relief model with hillshade from local relief model overlay (70% transparency). (d) Sky-view factor with hillshade overlay (70% transparency). From the Åsgarden site, Vega. Illustration: Kristoffer R. Rantala. [Colour figure can be viewed at [wileyonlinelibrary.com](https://onlinelibrary.wiley.com)]



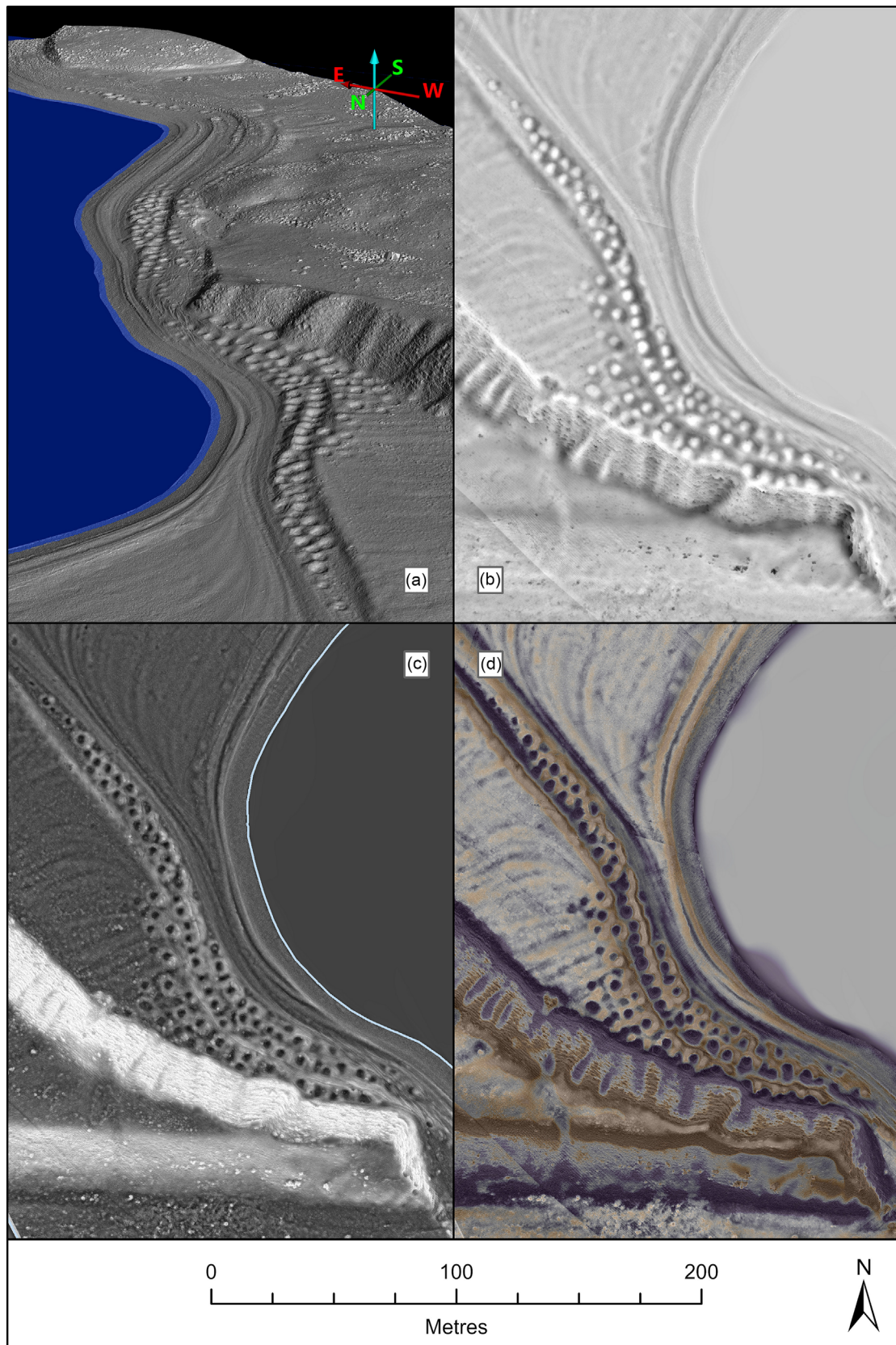


**FIGURE 13** Example II of visualization techniques applied during the study. (a) Quick Terrain Modeler. (b) Negative openness, ArcGIS. (c) Local dominance with slope overlay (70% transparency), ArcGIS. (d) Blend with local relief model as base, 50% sky-view factor, 30% hillshade and 30% slope. From the Wikirrh site on the Outer Peninsula, Cambaceres. Illustration: Kristoffer R. Rantala. [Colour figure can be viewed at [wileyonlinelibrary.com](https://onlinelibrary.wiley.com)]



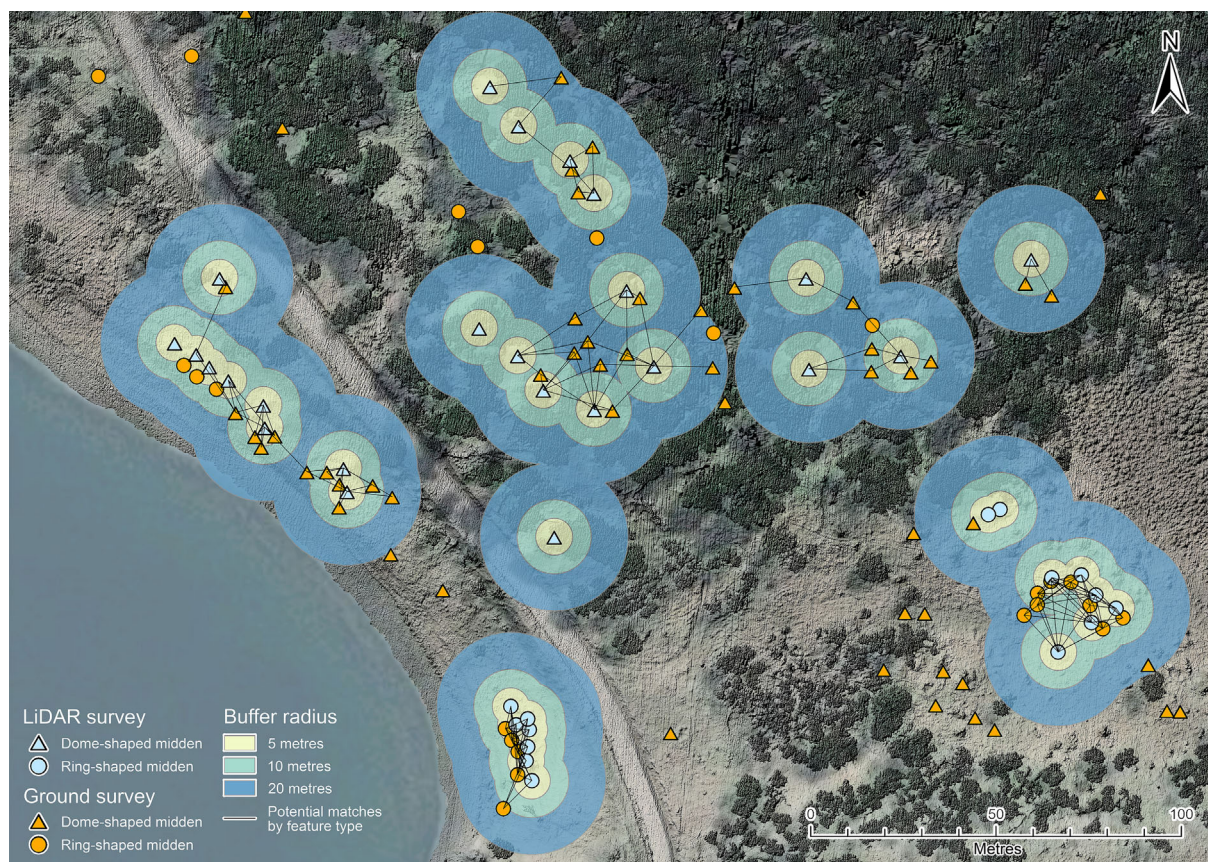


**FIGURE 14** The relatively low precision of the GPS data from the ground survey in Cambaceres made feature-to-feature comparison difficult. On the figure example, the lines only connect possible matches between LiDAR anomalies and recorded features of the same category, within a 20-m search radius (buffer) from the origin feature. The distance between possible matches is significantly increased in wooded areas, showing that a 20-m search radius is necessary for identifying matches in such areas. Illustration: Magnar M. Gran. [Colour figure can be viewed at [wileyonlinelibrary.com](https://onlinelibrary.wiley.com)]

A total of 58 anomalies interpreted as house pits were identified by LiDAR (Table 7). Eighteen of these were not previously scheduled, a number that falls to three if high confidence is emphasized. Within the ground survey elevation intervals, 36 anomalies interpreted as house pits were identified, of which 5 had no field match within a 20-m buffer radius. Most of the new possible identifications were located within Floaskaret-Skavdalen ( $n = 10$ ) and Åsgarden-Porsmyrdalen ( $n = 7$ ).

## 5 | DISCUSSION

The grand total success rates of 69% at Cambaceres and 78% on Vega are as expected inasmuch as similar results have been obtained in other studies scrutinizing detection success. In one study, 78% of features related to copper mining activities were identified (Gallagher & Josephs, 2008), while in two other cases from forested areas, the detection rates were reported to be 71% (Risbøl, 2010) and 61% (Bollandsås et al., 2012). Obviously, one must be cautious of making direct comparisons between studies because such results are affected by a range of factors, including topography, type and size of

structures, vegetation, data resolution and more. Nevertheless, the results seem to indicate an overall detection success rate of 60%–80%.

The comparative analyses from both case studies also show that a high number of LiDAR anomalies had no field match within a 20-m search radius. Provided that we accept the criteria for the search radius (refer to Section 3), there are only two ways of interpreting such findings: as false positives or as new identifications. As we have thorough field-verified data from both Cambaceres and Vega, it is reasonable to think that most of the LiDAR anomalies without a field match are false positives. However, given that the ground surveys were carried out before the LiDAR surveys, the answer is not so straightforward. Indeed, as we argue below, there is reason to believe that we have identified previously unknown features in both case study areas.

The results from the Cambaceres Bay case study suggest that a significant number of new ring-shaped middens were identified by the LiDAR survey, although the number is substantially lower than that indicated by Table 2. We only had the opportunity to check a limited number of possible ring-shaped identifications after the interpretation of the LiDAR data, and the field verifications suggest that more than



**TABLE 2** The number of LiDAR anomalies identified in each sub-area in total and only those with a high level of confidence, as well as how many of them were not recorded during the Cambaceres ground survey (No field match), in quantity and percentage. The columns labelled 'Total' show the quantity/percentage of matches between LiDAR anomalies and recorded features without taking feature category into account. The other columns only show the quantity/percentage of matches within the individual feature categories (ring-shaped middens, domes etc.).

Area	Description	All included						High confidence (3–4)					
		Total	TotBy FeatTy	RS	Do	CaRu	Spec	Total	TotBy FeatTy	RS	Do	CaRu	Spec
Varela Peninsula	LiDAR anomalies	142	142	135	7			83	83	83			
	No field match	73	79	74	5			19	23	23			
	No field match (%)	51	56	55	57			23	28				
Interior Binushmuka	LiDAR anomalies	182	182	106	73	3		70	70	67	3		
	No field match	11	11	10	1	0		0	0	0	0		
	No field match (%)	6	6	9	1	0		0	0	0	0		
Interior Imiwaia	LiDAR anomalies	135	135	101	33		1	81	81	67	13		1
	No field match	21	33	13	20		0	16	16	8	8		0
	No field match (%)	16	24	13	61		0	20	20	12	62		0
Central Peninsula	LiDAR anomalies	104	104	93	11			70	70	70			
	No field match	23	25	24	1			3	4	4			
	No field match (%)	22	24	26	9			4	6	6			
Outer Peninsula	LiDAR anomalies	345	345	331	14			273	273	267	6		
	No field match	105	105	98	7			40	41	41	0		
	No field match (%)	30	30	30	50			15	15	15	0		
Interior North	LiDAR anomalies	45	45	33	12			14	14	13	1		
	No field match	2	9	2	7			0	1	0	1		
	No field match (%)	4	20	6	58			0	7	0	100		
Interior Southeast	LiDAR anomalies	97	97	63	34			39	39	39			
	No field match	7	7	2	5			1	1	1			
	No field match (%)	7	7	3	15			3	3	3			
Exterior Southeast	LiDAR anomalies	60	60	43	17			24	24	22	2		
	No field match	11	22	18	4			5	5	3	2		
	No field match (%)	18	37	42	24			21	21	14	100		
Grand total	LiDAR anomalies	1110	1110	905	201	3	1	654	654	628	25	0	1
	No field match	253	290	241	49	0	0	84	91	80	11	0	0
	No field match (%)	23	26	27	24	0	0	13	14	13	44	0	0

Abbreviations: CaRu, canoe runway; Do, dome; RS, ring-shaped; Spec, special feature (Casa Grande); TotBy FeatTy, total by feature type.

three out of four anomalies are false positives. However, despite disproving anomalies interpreted as ring-shaped middens with a relatively high confidence, the field check also verified anomalies with low confidence as ring-shaped middens. If the remaining anomalies fall within the same pattern as the controlled data, it implies that more than 50 previously unknown ring-shaped middens were identified by the LiDAR survey.<sup>4</sup> These new LiDAR-identified ring-shaped features are primarily located within or close to the known main clusters, and most of them are very subtle circular depressions that can be hard to spot with the bare eye on the ground. Conversely, the LiDAR omissions of ring-shaped features from the ground survey record are

mostly small ones located *outside* the main clusters, higher up and farther away from the shore, in more densely vegetated areas.

In general, larger features are easier to identify than smaller ones when LiDAR models are interpreted (Risbøl et al., 2013). Nevertheless, such a statement is an oversimplification. Not only does size matter: Shape is also decisive for identification. Small features with a distinct geometric shape are easier to identify in a LiDAR data set than larger features without such characteristics (Emmitt et al., 2020; Risbøl et al., 2013; Roiha et al., 2021). Accordingly, small, subtle and hardly visible features ignored during fieldwork are often identifiable when observed from above on a LiDAR-generated model (Barbour et al., 2019; Casana et al., 2021; Davis et al., 2019). The relatively high success rate in terms of identifying subtle ring-shaped middens in Cambaceres is in accordance with this pattern.

<sup>4</sup> $(6/26) \times 241 = 55.6$ .



**TABLE 3** The number of features recorded in the Cambaceres Surveys, how many of them were not among the LiDAR identifications (LiDAR omissions) and a calculated success rate for the LiDAR survey based on these numbers. The first column, labelled 'Total', shows the quantity/percentage of matches between recorded features and LiDAR anomalies without taking feature category into account. The other columns only show the quantity/percentage of matches within the individual feature categories (ring-shaped middens, domes etc.).

Area	Description	Total	TotBy FeatTy	Ring-shaped			Dome					Other	
				Total	L	S	Total	XL	L	M	S	CaRu	Spec
Varela Peninsula	Ground survey	99	99	63	52	11	36	1	4	16	15		
	LiDAR omissions	30	36	3	0	3	33	1	4	14	14		
	Success rate (%)	70	64	95			8						
Interior Binushmuka	Ground survey	245	245	124	39	85	118	1	4	31	82	3	
	LiDAR omissions	71	71	23	5	18	48	0	2	14	32	0	
	Success rate (%)	71	71	81			59					100	
Interior Imiwaia	Ground survey	160	160	130	70	60	29	1	5	16	7		1
	LiDAR omissions	47	54	41	19	22	13	1	3	5	4		0
	Success rate (%)	71	66	68			55						100
Central Peninsula	Ground survey	140	140	81	64	17	59	9	13	22	15		
	LiDAR omissions	59	60	11	3	8	49	6	9	20	14		
	Success rate (%)	58	57	86			17						
Outer Peninsula	Ground survey	254	254	236	210	26	18			7	11		
	LiDAR omissions	14	14	3	0	3	11			0	11		
	Success rate (%)	94	94	99			39						
Interior North	Ground survey	74	74	56	31	25	18	4	4	8	2		
	LiDAR omissions	31	36	25	6	19	11	3	2	4	2		
	Success rate (%)	58	51	55			39						
Interior Southeast	Ground survey	174	174	86	33	53	88	10	12	47	19		
	LiDAR omissions	86	86	25	3	22	61	4	9	33	15		
	Success rate (%)	51	51	71			31						
Exterior Southeast	Ground survey	94	94	28	19	9	66	8	5	29	24		
	LiDAR omissions	44	55	2	1	1	53	4	2	23	24		
	Success rate (%)	53	41	93			20						
Grand total	Ground survey	1240	1240	804	518	286	432	34	47	176	175	3	1
	LiDAR omissions	382	412	133	37	93	279	19	31	113	116	0	0
	Success rate (%)	69	67	83	93	67	35	44	34	36	34	100	100

Abbreviations: CaRu, canoe runway; L, large; M, medium; S, small; Spec, special feature (Casa Grande); TotBy FeatTy, total by feature type; XL, very large.

**TABLE 4** Results from the field verification of a small selection of LiDAR anomalies identified as ring-shaped middens (sorted by confidence). None of these were recorded during the previous ground survey (the Cambaceres Surveys).

Confidence	Positive	Negative	Total
1 Low	3	7	10
2 Below medium	2	10	12
3 Above medium	1	3	3
4 High	0	0	0
Total	6	20	26

The detection success was considerably lower for dome-shaped than for ring-shaped middens. Although it is slightly better for very large domes than for the other categories, the largest omitted

dome-shaped structure measured 20 m × 10 m × 0.3 m (labelled hb637, in Bjerck, Zangrando, et al., 2016, appendix 1.1). In addition to its low height, it was reported to be heavily disturbed by cattle hooves. The 19 very large domes that were missed can be explained either by poor data (incomplete coverage and/or alignment), faulty vegetation filtering, location in rugged terrain, modern or natural disturbance (road, cattle and erosion), irregular shape and/or low height. On the other hand, it seems contradictory that small domes were identified at all by the LiDAR survey, particularly because they have been described as 'merely a patch of midden material on the ground (...) and not actual "dome" formations' (Bjerck, Zangrando, et al., 2016, p. 33).

The main reason for the significantly less successful results regarding domes appears to be that they are more frequently situated in areas with more vegetation and therefore less optimal conditions



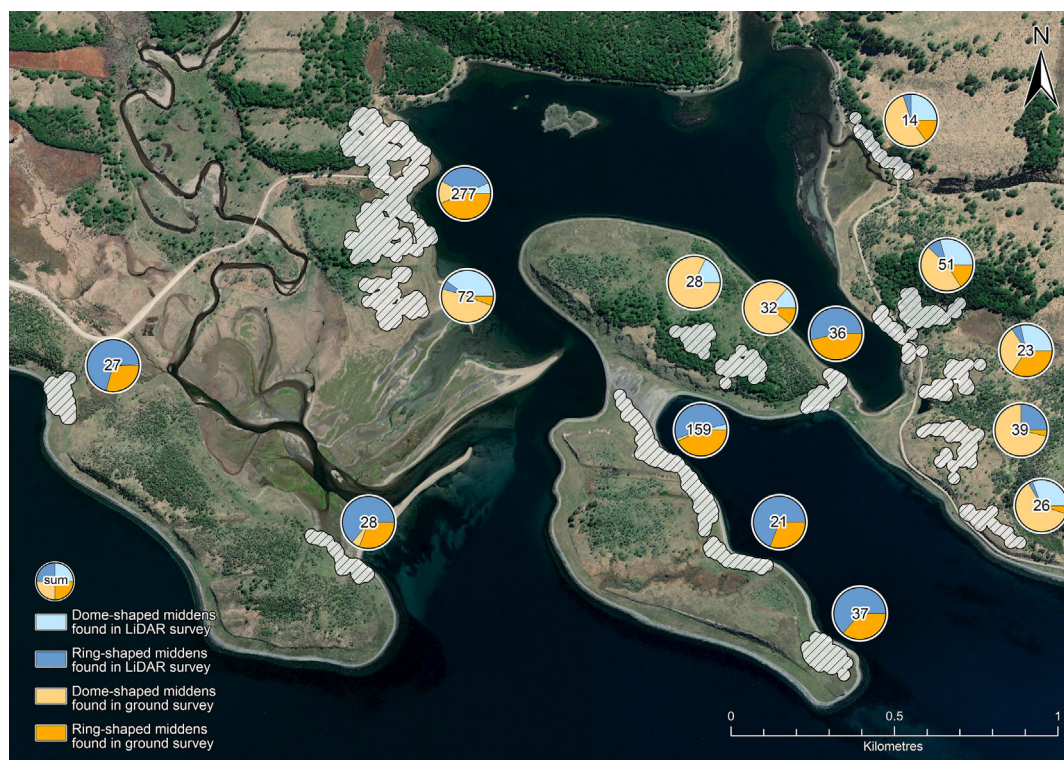


**FIGURE 15** Comparison of LiDAR identifications of ring- and dome-shaped middens with the ground survey record from 15 clusters in Cambaceres. The clusters were generated from dissolved buffer polygons using point features from both LiDAR anomalies and recorded features as the origin for creating the 20-m buffer polygons. The 15 largest polygons were compared. Illustration: Magnar M. Gran. [Colour figure can be viewed at [wileyonlinelibrary.com](https://onlinelibrary.wiley.com/doi/10.1002/arj.1918)]

for LiDAR mapping compared with open areas closer to the shoreline (see Table 5 and Figure 15). That a dense canopy and/or low vegetation prevent laser light from reaching the ground is a well-known challenge within archaeological LiDAR use (Doneus et al., 2022). Even though one of the greatest advantages of LiDAR is its ability to penetrate vegetation, very dense vegetation remains a limiting factor. Another explanation for the disparity between the success rates between dome- and ring-shaped features is that it generally seems harder to identify small convex features (like domes and other mounds) than small and subtle concave features (like pits and depressions). This may be related to how the filtering algorithms work: They are set to identify and filter away vegetation above the ground surface without always managing to differentiate between what are and what are not human-made features (Masini et al., 2022). In practice, there are also many more viable explanations for whatever is heaped on the surface compared with what has cut through it.

In that respect, it should also be underscored that distinguishing between dome- and ring-shaped middens can be a matter of interpretation, depending on whether one recognizes a minor depression next to a dome-shaped midden as an archaeological trace of a dwelling foundation. If one's answer is 'no', the midden is interpreted as a dome; if 'yes', it may just as well be categorized as a ring-shaped midden. As argued above, subtle depressions may also be easier to recognize when applying powerful visualization techniques on LiDAR images than in the field.

On Vega, the results indicate that LiDAR was quite successful in detecting pit features, to be more precise, Mesolithic house pits. The survey might have identified as many as 18 new house pits (mostly outside the areas covered by the ground survey), even though they are situated in rather rugged terrain and do not necessarily appear as house pits when observed from the ground. Ironically, the main reason why we should be optimistic about our results is that 13 of the new identifications are located in the more randomly surveyed terrain *outside* the targeted elevation intervals of the intensive ground survey (cf. Bjerck, 1989) (Figure 16). Nevertheless, it should be underscored that the LiDAR data were not easy to interpret and before they are proved in the field, there is a risk that many of the anomalies are false positives.

The encouraging results from Vega seem to support the experiences gained from the Stone Age Demographics project, where LiDAR was used to identify Mesolithic house pits in coastal landscapes in the far north of Norway (Damm et al., 2021; Damm & Skandfer, 2021). One major challenge with applying LiDAR to study the Mesolithic is that most archaeological traces are not visible above ground. Not even pit houses are all visible on the surface due to post-occupational processes, such as peat accumulation (Åstveit et al., 2008; Fretheim, 2019). Thus, it is easy to understand why LiDAR has mainly been employed for palaeo-landscape modelling in Mesolithic studies. However, pit houses represent an important marker and step towards a more sedentary lifestyle (Bjerck, 1990), and although the rapid

**TABLE 5** Results from comparison of LiDAR identifications and the ground survey record from 15 clusters in Cambaceres, including the main characteristics of the clusters based on feature and landscape type. The table shows how many of the LiDAR anomalies had no match of the same feature type within 5-, 10- and 20-m search radiuses, respectively. It also shows that the number of matches increased significantly for domes and wooded areas particularly when the search radius was increased from 10 to 20 m, justifying the use of 20 m as the search radius.

Cluster	Feature types	Landscape	LiDAR identifications	No match 5 m	No match 10 m	No match 20 m
5	Domes mostly	Open	60	21	0	0
16	Ring-shaped	Open	42	14	8	6
17	Domes	Wooded	5	0	0	0
20	Both	Open	12	8	4	0
22	Domes mostly	Mostly wooded	31	13	2	0
33	Ring-shaped	Open	65	46	38	38
34	Ring-shaped	Open	197	44	38	38
36	Ring-shaped	Open	47	34	26	26
37	Ring-shaped	Open	65	36	28	28
38	Domes mostly	Wooded	5	1	0	0
40	Domes mostly	Sparsely wooded	13	8	3	0
41	Domes mostly	Open	13	2	0	0
42	Domes mostly	Wooded	6	5	3	0
43	Ring-shaped mostly	Open/sparsely wooded	206	51	4	0
44	Ring-shaped mostly	Open	50	24	22	22
Total			817	307	176	158
Percentage			100	38	22	19
<b>Match increase from search radius expansion</b>						
	<b>Category</b>	<b>Clusters</b>		<b>5 to &gt;10 m</b>	<b>10 to &gt;20 m</b>	
	Wooded	17, 22, 38, 40 and 42		32%	13%	
	Open	5, 16, 20, 33, 34, 36, 37, 41 and 42		12%	1%	
	<b>Ratio wooded–Open</b>			<b>2.7</b>	<b>12.2</b>	
	Domes	5, 17, 22, 38, 40, 41 and 42		32%	6%	
	Ring-shaped	16, 33, 34, 36, 37, 43 and 44		13%	1%	
	<b>Ratio domes–Ring-shaped</b>			<b>2.5</b>	<b>6.7</b>	

**TABLE 6** The number of recorded features within the three study areas on Vega, the numbers that were not among the LiDAR identifications ('LiDAR omissions') and a calculated success rate for the LiDAR survey based on these numbers. While the comparison in the 'Total' column is based on all recorded features, the 'Verified features' column counts omissions and calculates the success rate based on verified features only.

Area	Description	Total	Verified features
Åsgarden–Porsmyrdalen	Ground survey	36	29
	LiDAR omissions	7	3
	Success rate (%)	81	90
Floaskaret–Skavdalen	Ground survey	10	7
	LiDAR omissions	2	1
	Success rate (%)	80	86
Middagskarheia–Hammaren	Ground survey	5	4
	LiDAR omissions	2	1
	Success rate (%)	60	75
Grand total	Ground survey	51	40
	LiDAR omissions	11	5
	Success rate (%)	78	88



**TABLE 7** The number of LiDAR anomalies identified in each of the three study areas on Vega in total and only those with a high level of confidence, as well as how many of them were not recorded during the previous ground survey ('No field match'), in quantity and percentage. The columns under 'Ground Surv area' apply the elevation intervals for the ground survey as the basis for the comparison. The columns under 'LiDAR Surv area' apply the limits of the LiDAR survey as the basis for the comparison and, consequently, the included areas that were randomly surveyed in the comparison. In the 'LiDAR Surv area' columns, it is the number of LiDAR identifications that is most interesting, and not the number of matches.

Area	Description	Ground Surv area		LiDAR Surv area	
		Total	HiConf (3–4)	Total	HiConf (3–4)
Åsgarden–Porsmyrdalen	LiDAR anomalies	28	15	36	20
	No field match	2	0	7	3
	No field match (%)	7	0	19	15
Floaskaret–Skavdalen	LiDAR anomalies	7	2	18	3
	No field match	3	1	10	0
	No field match (%)	43	50	56	0
Middagskarheia–Hammaren	LiDAR anomalies	1	1	4	1
	No field match	0	0	1	0
	No field match (%)	0	0	25	0
Grand total	LiDAR anomalies	36	18	58	24
	No field match	5	1	18	3
	No field match (%)	14	6	31	13

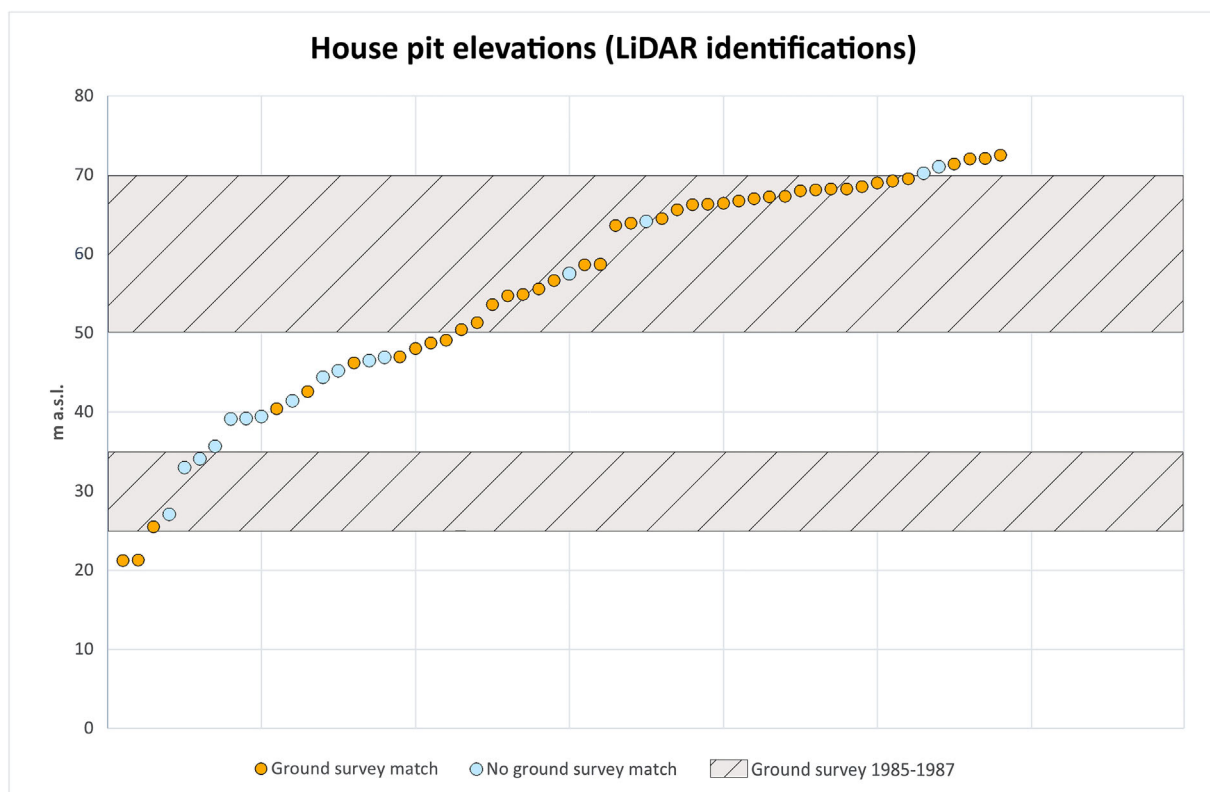


**FIGURE 16** LiDAR identifications on Vega based on elevation. LiDAR anomalies with no field match are mostly located outside the elevation intervals that were intensively surveyed by Bjerk (1989). Illustration: Jo Sindre P. Eidshaug. [Colour figure can be viewed at [wileyonlinelibrary.com](https://onlinelibrary.wiley.com)]

accumulation of house pits in the Norwegian archaeological record in the past couple of decades has mostly resulted from development-led archaeological projects, they have been recognized as ‘part of common practices rather than isolated, exceptional phenomena’ (Fretheim, 2019, p. 15). For more systematic, supra-regional studies of Late Mesolithic settlement patterns and landscape use, LiDAR can be a most useful, time-efficient tool.

Finally, it is also evident that LiDAR will bring something to the table for coastal archaeology apart from identifying new features. We will briefly look into a few examples based on ongoing discussions from Tierra del Fuego. Overall, the LiDAR survey seems to support some of the general trends that were observed by the Cambaceres Surveys (cf. Bjerck, Zangrando, et al., 2016, pp. 75–77). For instance, there is an interesting difference in the distribution pattern of ring- and dome-shaped middens. Whereas ring-shaped middens are mostly located in clusters close to the beach—even below the marine ridge at about 5 m a.s.l. (cf. Zangrando et al., 2016)—domes are usually located farther up, at some distance from the beach (Figures 15 and 17). Moreover, regarding the formation of the aggregations of ring-shaped shell middens, it was observed that the middens that were located at the outskirts of the aggregations had lower walls than those in the

middle. Accordingly, the aggregations expanded over time as new dwelling huts were raised immediately outside the older structures, presumably to take advantage of the shelter they provided (Bjerck, Zangrando, et al., 2016, p. 75; see also Piana & Orquera, 2010). Our new LiDAR identifications of subtle ring-shaped middens close to the known aggregations seem to support this expansion pattern. Occasionally, they seem to have expanded in several directions and with small interruptions, but mostly, they have accumulated like pearls on a string along the contemporary shoreline. This conclusion is also consistent with the idea that the shell middens themselves acted as a major attractor for new settlements (Piana & Orquera, 2010; Zangrando, 2018).

The LiDAR data can also shed light on the discussion pertaining to the extent of site preparation prior to the construction of the dwelling huts. In a 19th-century Yagan–English dictionary (Bridges, 1987), we read:

*ū[luš]wāna* tr. To clear a site for a wigwam [i.e., dwelling hut] floor. (...) To clear away for a floor a house. (...)  
*ū[luš]w[önd]eka* tr. To make a hollow all ready for the erection of a wigwam. (Bridges, 1987, p. 92)

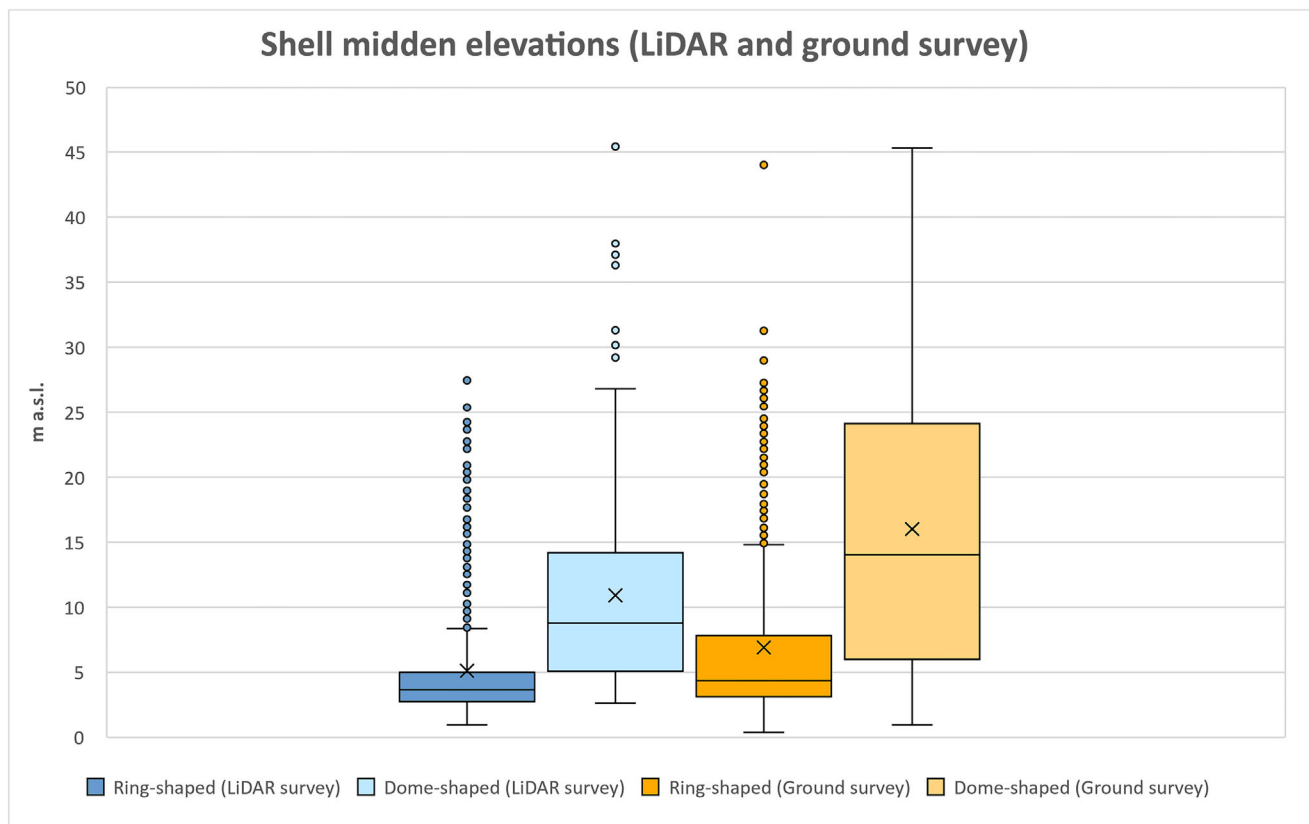


**FIGURE 17** Box diagram showing the distribution of ring- and dome-shaped middens identified on LiDAR and recorded in the ground survey in Cambaceres based on elevation. There is an obvious distinction between the location of ring- and dome-shaped middens in the landscape, the former category being mostly located below the marine ridge and the latter being located higher up. Note that although the z-values from the ground survey GPS coordinates were extracted from the digital terrain model, the coordinates per se may be erroneous due to low GPS accuracy (see Section 3; Bjerck, Zangrando, et al., 2016), affecting the distribution. Illustration: Jo Sindre P. Eidshaug. [Colour figure can be viewed at [wileyonlinelibrary.com](https://onlinelibrary.wiley.com)]



*mõtātānunata* i. To become clear earth unmixed or no more covered with grass as the floor of a wigwam when the grass is removed. (Bridges, 1987, p. 334)

Although some accounts based on ethnographic evidence claim that the Fuegians occasionally used to *dig pits* as part of preparing a foundation for their huts (e.g., Bird, 1938; Lothrop, 1928, p. 128; for an overview, see Orquera & Piana, 1989–1990, pp. 60–61), the archaeological evidence shows that the ring-shaped shell midden walls formed around huts were erected *on the surface* (Orquera & Piana, 1989–1990, 2009; Piana & Orquera, 2010; see also Bjerck, Zangrando, et al., 2016, p. 30). Judging by the LiDAR data, the latter is certainly the norm. This is also the case for the subtle depressions discussed above, as they have no actual pits (including those that were subsequently verified in the field). While we believe these are remains of dwelling foundations just like the other ring-shaped structures, the depressions may simply have resulted from trampling or other activities inside the dwellings. On the other hand, there are also a fairly significant number of ring-shaped middens with bases situated 30–40 cm below the natural ground level in the 3D data, which indicate intentional preparation or modification of the site by means of digging (Figure 18). Although this diversity does seem to support the theory suggested by both the dictionary (Bridges, 1987) and the Cambaceres

Surveys report (Bjerck, Zangrando, et al., 2016) that one practice does not necessarily rule out the other, we would like to stress that archaeological excavations in those newly identified cases are imperative for concluding on this matter.

## 6 | CONCLUSION

This paper has shown variable detection success between the case study areas. On Vega, we identified most of the known house pits and some possible new ones in less intensively surveyed areas, a result that was far better than expected. Cambaceres proved more challenging and we experienced a significant disparity in success rates between the two types of structures. However, the results are in accordance with conclusions from previous similar studies, where small features and/or features without a distinct shape proved hard to identify on LiDAR-generated images. This is especially true of features situated in environments whose vegetation posed challenges, like dense foliage. To create a very detailed DTM, one needs a dense set of ground points, and it is questionable whether improvements could be obtained by testing additional data-processing algorithms and filtering techniques. This is beyond the scope of this paper but is mentioned here as the basis of a possible additional study using the collected data.

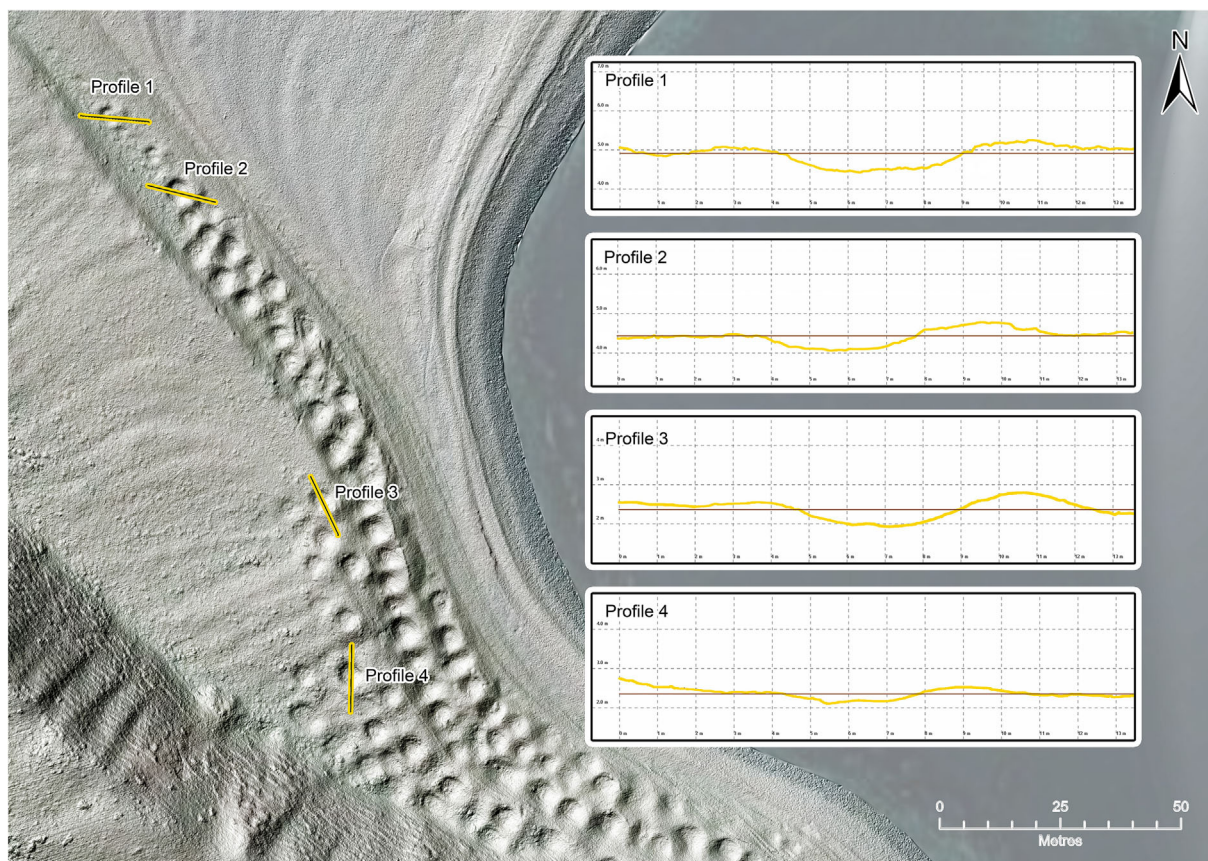


**FIGURE 18** Profile views of a selection of ring-shaped middens with bases below the natural ground at Wikirrh, Outer Peninsula, Cambaceres, possibly indicating that some of the dwelling huts were placed in pits that were dug as part of the site preparation. Illustration: Magnar M. Gran. [Colour figure can be viewed at [wileyonlinelibrary.com](https://onlinelibrary.wiley.com/doi/10.1111/1522-2575.12521)]

In any case, the study produced fairly good results and important experiences that are of great value for future large-scale mappings in both regions. It is evident that UAV LiDAR can contribute to coastal landscape archaeology and that its added value is not limited to identifying new features. Most of all, it is both flexible and time efficient, of benefit to landscape-scale studies. There is also the potential to conduct further studies using the LiDAR data, such as volume calculations of midden materials, to study site formation processes and to conduct demographic studies, as occurs in other regions with shell middens across the world. Furthermore, LiDAR data can be used for more than just archaeological purposes in such regions; for instance, they can provide a basis for cross-disciplinary environmental, topographical and geomorphological studies.

## ACKNOWLEDGEMENTS

The Marine Ventures project was supported by the Research Council of Norway. We would like to thank the Centro Austral de Investigaciones Científicas/Consejo Nacional de Investigaciones Científicas y Técnicas (CADIC-CONICET), Argentina, and the Department of Archaeology and Cultural History at the Norwegian University of Science and Technology (NTNU) University Museum, Norway, for financial and practical aid. Without their support, we would not have been able to conduct this study. Fieldwork was partially supported by PICT 2017 1230 (PICT - Agencia I+D+i: Proyectos de Investigación Científica y Tecnológica, Agencia Nacional de Promoción de la Investigación, el Desarrollo Tecnológico y la Innovación). We thank Martín Castro, Adalberto Ferlito and Juan Manuel Bareiro for the help they provided in connection with field activities.

## CONFLICT OF INTEREST STATEMENT

The authors declare no conflicts of interest.

## DATA AVAILABILITY STATEMENT

The data that support the findings of this study are available from the corresponding author upon reasonable request.

## ORCID

Ole Risbøl  <https://orcid.org/0000-0003-1891-1868>

## REFERENCES

- Adamopoulos, E., & Rinaudo, F. (2020). UAS-based archaeological remote sensing: Review, meta-analysis and state-of-the-art. *Drones*, 4(3), 46. <https://doi.org/10.3390/drones4030046>
- Álvarez, M., Fiore, D., Tivoli, A., Salvatelli, L., Saletta, M. J., & Briz, I. (2013). Variabilidad de actividades humanas en momentos recientes de la ocupación del canal Beagle (Tierra del Fuego): El caso de Lanashuaia XXI. In A. F. Z. Zangrando, R. Barberena, A. Gil, G. Neme, M. Giardina, L. Luna, C. Otaola, S. Paulides, L. Salgán, & A. Tivoli (Eds.), *Tendencias teórico-metodológicas y casos de estudio en la arqueología de la Patagonia* (pp. 559–568). Sociedad Argentina de Antropología y Museo de Historia Natural de San Rafael.
- Åstveit, L. I., Meling, T., Gundersen, J., Jørgensen, G., & Normann, S. (2008). In H. B. Bjerck (Ed.), *Ormen Lange Nyhamna: NTNU Vitenskapsmuseets arkeologiske undersøkelser*. Tapir Akademisk.
- Barbour, T. E., Sassaman, K. E., Almeyda Zambrano, A. M., Broadbent, E. N., Wilkinson, B., & Kanaski, R. (2019). Rare pre-Columbian settlement on the Florida Gulf Coast revealed through high-resolution drone LiDAR. *PNAS*, 116(47), 23493–23498. <https://doi.org/10.1073/pnas.1911285116>
- Barceló, J. A., Piana, E. L., & Martinioni, D. R. (2002). Archaeological spatial modelling. A case study from Beagle Channel (Argentina). In G. Burenhult (Ed.), *Archaeological informatics: Pushing the envelope*. CAA 2001, Computer Applications and Quantitative Methods in Archaeology. Proceedings of the 29<sup>th</sup> Conference, Gotland, April 2001. BAR International Series 1016, 2002. (pp. 351–360). Oxford: Archaeopress.
- Bird, J. (1938). Antiquity and migrations of the early inhabitants of Patagonia. *Geographical Review*, 28, 250–275. <https://doi.org/10.2307/210474>
- Bjerck, H. B. (1989). Forskningsstyrt kulturminneforvaltning på Vega, Nordland. En studie av steinaldermenneskenes boplassmønstre og arkeologiske letemetoder. *Gunneria*, 61, 1–212.
- Bjerck, H. B. (1990). Mesolithic site types and settlement patterns at Vega. *Acta Archaeologica*, 1989(60), 1–32.
- Bjerck, H. B. (2007). Mesolithic coastal settlements and shell middens (?) in Norway. In N. Milner, O. E. Craig, & G. N. Bailey (Eds.), *Shell middens in Atlantic Europe* (pp. 5–30). Oxbow.
- Bjerck, H. B. (2008). Norwegian Mesolithic trends: A review. In G. N. Bailey & P. Spikins (Eds.), *Mesolithic Europe* (pp. 60–106). Cambridge University Press.
- Bjerck, H. B., Breivik, H. M., Fretheim, S. E., Piana, E. L., Skar, B., Tivoli, A. M., & Zangrando, A. F. J. (Eds.). (2016). *Marine ventures: Archaeological perspectives on human-sea relations*. Equinox.
- Bjerck, H. B., Eidshaug, J. S. P., Risbøl, O., Breivik, H. M., & Zangrando, A. F. J. (2019). Struts og drone: Fra årets feltarbeid på Ildlandet i Argentina. *SPOR—Nytt Fra Fortiden*, 34(1), 37–43.
- Bjerck, H. B., & Zangrando, A. F. (2013). Marine ventures: Comparative perspectives on the dynamics of early human approaches to the seascapes of Tierra del Fuego and Norway. *The Journal of Island and Coastal Archaeology*, 8(1), 79–90. <https://doi.org/10.1080/15564894.2012.756083>
- Bjerck, H. B., Zangrando, A. F. J., Breivik, H. M., Piana, E., & Negre, J. (2016). *Marine ventures: The Cambaceres Surveys, Tierra del Fuego, Argentina*. NTNU Vitenskapsmuseet arkeologisk rapport 2016-15.
- Bollandsås, O. M., Risbøl, O., Ene, L. T., Nesbakken, A., Gobakken, T., & Næsset, E. (2012). Using airborne small-footprint laser scanner data for detection of cultural remains in forests: An experimental study of the effects of pulse density and DTM smoothing. *Journal of Archaeological Science*, 39, 2733–2743. <https://doi.org/10.1016/j.jas.2012.04.026>
- Breivik, H. M. (2016). *Dynamic relations between humans and environment in the earliest settlement phase of Norway (9500–8000 cal BC)* [Unpublished doctoral thesis]. Norwegian University of Science and Technology (NTNU).
- Bridges, T. (1987). *Yamana-English: A dictionary of the speech of Tierra del Fuego*. Zagier y Urrutu.
- Butto, A., Saletta, M. J., & Fiore, D. (2018). Cultura visual de cazadores Shelk'nam/Haush y Yámana/Yagán de Tierra del Fuego: Una comparación entre fotografías, textos y artefactos arqueológicos. *Nuevo Mundo Mundos Nuevos* [online]. <https://doi.org/10.4000/nuevomundo.72853>
- Campana, S. (2017). Drones in archaeology. State-of-the-art and future perspectives. *Archaeological Prospection*, 24(4), 275–296. <https://doi.org/10.1002/arp.1569>
- Casana, J., Laugier, E. J., Hill, A. C., Reese, K. M., Ferwerda, C., McCoy, M. D., & Ladefoged, T. (2021). Exploring archaeological landscapes using drone-acquired lidar: Case studies from Hawai'i, Colorado, and New Hampshire, USA. *Journal of Archaeological Science: Reports*, 39, 103133. <https://doi.org/10.1016/j.jasrep.2021.103133>



- Crutchley, S. (2009). Using LiDAR in archaeological contexts: The English heritage experience and lessons learned. In G. L. Heritage & A. R. G. Large (Eds.), *Laser scanning for the environmental sciences* (pp. 180–200). Blackwell. <https://doi.org/10.1002/9781444311952.ch12>
- Damm, C., & Skandfer, M. (2021). Rapport fra befarings på Seiland, Slettnes og langs Vargsundet i 2018 under forskningsprosjektet “Stone Age Demographics”. *Serpentino Reports*, 3, 1–46. <https://doi.org/10.7557/7.5771>
- Damm, C., Skandfer, M., & Vollan, K. W. B. (2021). Rapport fra befarings og registrering på Fella, Vatnan og Gåshopen i Hammerfest kommune, Finnmark fylke 2019. *Serpentino Reports*, 3, 1–88. <https://doi.org/10.7557/7.5795>
- Davis, D. S., Caspari, G., Lipo, C. P., & Sanger, M. C. (2021). Deep learning reveals extent of Archaic Native American shell-ring building practices. *Journal of Archaeological Science*, 132, 105433. <https://doi.org/10.1016/j.jas.2021.105433>
- Davis, D. S., DiNapoli, R., Sanger, M. C., & Lipo, C. P. (2020). The integration of lidar and legacy datasets provides improved explanations for the spatial patterning of shell rings in the American Southeast. *Advances in Archaeological Practice*, 8(4), 361–375. <https://doi.org/10.1017/aap.2020.18>
- Davis, D. S., Lipo, C. P., & Sanger, M. C. (2019). A comparison of automated object extraction methods for mound and shell-ring identification in coastal South Carolina. *Journal of Archaeological Science: Reports*, 23, 166–177. <https://doi.org/10.1016/j.jasrep.2018.10.035>
- Doneus, M., Banaszek, L., & Verhoeven, G. J. (2022). The impact of vegetation on the visibility of archaeological features in airborne laser scanning datasets from different acquisition dates. *Remote Sensing*, 14(4), 858. <https://doi.org/10.3390/rs14040858>
- Doneus, M., Doneus, N., Briese, C., Pregarbauer, M., Mandlbürger, G., & Verhoeven, G. (2013). Airborne laser bathymetry—Detecting and recording submerged archaeological sites from the air. *Journal of Archaeological Science*, 40(4), 2136–2151. <https://doi.org/10.1016/j.jas.2012.12.021>
- Doneus, N., Miholjek, I., Džin, K., Doneus, M., Dugonjić, P., & Schiel, H. (2020). Archaeological prospection of coastal and submerged settlement sites: Re-evaluation of the Roman site complex of Vižula, Croatia. *Archaeologia Austriaca*, 104, 253–281. <https://doi.org/10.1553/archaeologia104s253>
- Emmitt, J., Allely, K., Davies, B., Hoffman, E., & Holdaway, S. J. (2020). Preliminary archaeological survey and remote-sensing of shell mounds at Kwokkunum, Albatross Bay, Cape York Peninsula, Australia. *Queensland Archaeological Research*, 23, 9–24. <https://doi.org/10.25120/qar.23.2020.3718>
- Fiore, D., Butto, A., & Saletta, M. J. (2021). Tres miradas. Una comparación de los artefactos de caza, pesca y recolección de los Pueblos Originarios de Tierra del Fuego a partir de los registros arqueológico, fotográfico y escrito (siglos XVI al XX). *Revista Española de Antropología Americana*, 51, 187–202. <https://doi.org/10.5209/reaa.72794>
- Fiore, D., Saletta, M. J., & Varela, L. V. (2014). Digging photos and excavating sites. A comparative exploration of material culture patterns in ethnographic photographs and archaeological sites of Shelk’nam, Yamana and Alakaluf peoples from the Fuegian archipelago (Southern South America, 16th to 20th centuries). *Arctic & Antarctic*, 8, 69–128.
- Fretheim, S. E. (2017). *Mesolithic dwellings. An empirical approach to past trends and present interpretations in Norway* [Unpublished doctoral thesis]. Norwegian University of Science and Technology (NTNU).
- Fretheim, S. E. (2019). Discovering dwellings: A study of Late Mesolithic dwelling practices, contexts and attributes based on evidence from Central Norway. *Acta Archaeologica*, 90(1), 15–38. <https://doi.org/10.1111/16000390-09001003>
- Fretheim, S. E., Bjerck, H. B., Breivik, H. M., & Zangrando, A. F. J. (2018). Tent, hut or house? A discussion on Early Mesolithic dwellings proceeding from the site Mohalsen 2012-II, Vega, Northern Norway. In H. P. Blankholm (Ed.), *The early economy and settlement in Northern Europe—Pioneering, resource use, coping with change* (pp. 207–230). Equinox.
- Gallagher, J. M., & Josephs, R. L. (2008). Using LiDAR to detect cultural resources in a forested environment: An example from Isle Royale National Park, Michigan, USA. *Archaeological Prospection*, 15, 187–206. <https://doi.org/10.1002/arp.333>
- Guyot, A., Hubert-Moy, L., & Lorho, T. (2018). Detecting Neolithic burial mounds from LiDAR-derived elevation data using a multi-scale approach and machine learning techniques. *Remote Sensing*, 10(2), 225. <https://doi.org/10.3390/rs10020225>
- Hesse, R. (2010). LiDAR-derived local relief models—A new tool for archaeological prospection. *Archaeological Prospection*, 17, 67–72. <https://doi.org/10.1002/arp.374>
- Hesse, R. (2016). Visualisierung hochauflösender Digitaler Geländemodelle mit LiVT. In U. Lieberwirth & I. Herzog (Eds.), *Computeranwendungen und quantitative Methoden in der Archäologie*. 4. Workshop der AG CAA und des Exzellenzclusters Topoi 2013. (pp. 109–128). Topoi.
- Khan, S., Aragão, L., & Iriarte, J. (2017). A UAV–lidar system to map Amazonian rainforest and its ancient landscape transformations. *International Journal of Remote Sensing*, 38(8–10), 2313–2330. <https://doi.org/10.1080/01431161.2017.1295486>
- Kokalj, Ž., & Somrak, M. (2019). Why not a single image? Combining visualizations to facilitate fieldwork and on-screen mapping. *Remote Sensing*, 11(7), 747. <https://doi.org/10.3390/rs11070747>
- Lothrop, S. K. (1928). *The Indians of Tierra del Fuego. An account of the Ona, Yaghan, Alacaluf and Haush Natives of the Fuegian Archipelago*. Museum of the American Indian Heye Foundation. <https://doi.org/10.5479/sil.472342.39088016090599>
- Masini, N., Abate, N., Gizzi, F. T., Vitale, V., Minervino Amodio, A., Sileo, M., Biscione, M., Lasaponara, R., Bentivenga, M., & Cavalcante, F. (2022). UAV LiDAR based approach for the detection and interpretation of archaeological micro topography under canopy—The rediscovery of Peticara (Basilicata, Italy). *Remote Sensing*, 14, 6074. <https://doi.org/10.3390/rs14236074>
- McCoy, M. D., Casana, J., Hill, A. C., Laugier, E. J., & Ladefoged, T. N. (2022). Mapping ancient architecture via unpiloted aerial vehicle-acquired lidar: A case study of Hölualoa Royal Centre, Kona District, Hawaii Island. *The Journal of the Polynesian Society*, 131(1), 71–92. <https://doi.org/10.15286/jps.131.1.71-92>
- Mihu-Pintilie, A., Braşoveanu, C., & Stoleriu, C. C. (2022). Using UAV survey, high-density LiDAR data and automated relief analysis for habitation practices characterization during the Late Bronze Age in NE Romania. *Remote Sensing*, 14, 2466. <https://doi.org/10.3390/rs14102466>
- Monterroso-Checa, A., Moreno-Escribano, J. C., Gasparini, M., Conejo-Moreno, J. A., & Dominguez-Jiménez, J. L. (2021). Revealing archaeological sites under Mediterranean forest canopy using LiDAR: El Viandar Castle (*husum*) in El Hoyo (Belmez-Córdoba, Spain). *Drones*, 5, 72. <https://doi.org/10.3390/drones5030072>
- Murtha, T., Broadbent, E. N., Golden, C., Scherer, A., Schroder, W., Wilkinson, B., & Zambrano, A. (2019). Drone-mounted lidar survey of Maya settlement and landscape. *Latin American Antiquity*, 30(3), 630–636. <https://doi.org/10.1017/laq.2019.51>
- Optiz, R. (2016). Airborne laserscanning in archaeology: Maturing methods and democratizing applications. In M. Forte & S. Campana (Eds.), *Digital methods and remote sensing in archaeology: Archaeology in the age of sensing* (pp. 35–50). Springer, Cham. [https://doi.org/10.1007/978-3-319-40658-9\\_2](https://doi.org/10.1007/978-3-319-40658-9_2)
- Orquera, L. A., Legoupil, D., & Piana, E. L. (2011). Littoral adaptation at the southern end of South America. *Quaternary International*, 239, 61–69. <https://doi.org/10.1016/j.quaint.2011.02.032>
- Orquera, L. A., & Piana, E. L. (1989–1990). La formación de los montículos arqueológicos de la región del canal Beagle. *Runa*, 19, 59–90.
- Orquera, L. A., & Piana, E. L. (1999). *Arqueología de la región del canal Beagle (Tierra del Fuego, República Argentina)*. Sociedad Argentina de Antropología.
- Orquera, L. A., & Piana, E. L. (2009). Sea nomads of the Beagle Channel in the southernmost South America: Over six thousand years of coastal

- adaptation and stability. *The Journal of Island and Coastal Archaeology*, 4(1), 61–81. <https://doi.org/10.1080/15564890902789882>
- Orquera, L. A., & Piana, E. L. (2015). *La vida material y social de los Yámana*. Monte Olivia.
- Piana, E. L., & Canale, G. (1993–1994). Túnel II: Un yacimiento de la Fase Reciente del canal Beagle. *Relaciones de la Sociedad Argentina de Antropología*, 19, 363–389.
- Piana, E. L., & Orquera, L. A. (2010). Shellmidden formation at the Beagle Channel (Tierra del Fuego, Argentine). In D. Caladao, M. Baldia, & M. Boulanger (Eds.), *Monumental questions: Prehistoric megaliths, mounds, and enclosures*. BAR International Series 2122. (pp. 263–271). Archaeopress.
- Randall, A. R. (2014). LiDAR-aided reconnaissance and reconstruction of lost landscapes: An example of freshwater shell mounds (ca. 7500–500 cal b.p.) in northeastern Florida. *Journal of Field Archaeology*, 39(2), 162–179. <https://doi.org/10.1179/0093469014Z.00000000080>
- Risbøl, O. (2010). Towards an improved archaeological record through the use of airborne laser scanning. In M. Forte, S. Campana, & C. Liuzza (Eds.), *Space, time and place*. 3rd International Conference on Remote Sensing in Archaeology. British Archaeological Review, International Series 2118. (pp. 105–112). Archaeopress.
- Risbøl, O., Bollandsås, O. M., Nesbakken, A., Ørka, H. O., Næsset, E., & Gobakken, T. (2013). Interpreting cultural remains in airborne laser scanning generated digital terrain models: Effects of size and shape on detection success rates. *Journal of Archaeological Science*, 40, 4688–4700. <https://doi.org/10.1016/j.jas.2013.07.002>
- Risbøl, O., & Gustavsen, L. (2018). LiDAR from drones employed for mapping archaeology—Potential, benefits and challenges. *Archaeological Prospection*, 25, 329–338. <https://doi.org/10.1002/arp.1712>
- Roiha, J., Heinara, E., & Holopainen, M. (2021). The hidden cairns—A case study of drone-based ALS as an archaeological site survey method. *Remote Sensing*, 13(10), 2010. <https://doi.org/10.3390/rs13102010>
- Sánchez Díaz, F., García Sanjuán, L., & Rivera Jiménez, T. (2022). Potential and limitations of LiDAR altimetry in archaeological survey: Copper Age and Bronze Age settlements in southern Iberia. *Archaeological Prospection*, 29(4), 525–544. <https://doi.org/10.1002/arp.1869>
- Schroder, W., Murtha, T., Broadbent, E. N., & Almeida Zambrano, A. M. (2021). A confluence of communities: Households and land use at the junction of the Upper Usumacinta and Lacantún Rivers, Chiapas, Mexico. *World Archaeology*, 53(4), 688–715. <https://doi.org/10.1080/00438243.2021.1930135>
- Schülke, A. (Ed.). (2020). *Coastal landscapes of the Mesolithic: Human engagement with the coast from the Atlantic to the Baltic Sea*. Routledge. <https://doi.org/10.4324/9780203730942>
- Storch, M., Jarmer, T., Adam, M., & de Lange, N. (2022). Systematic approach for remote sensing of historical conflict landscapes with UAV-based laserscanning. *Sensors*, 22(1), 217. <https://doi.org/10.3390/s22010217>
- VanValkenburgh, P., Cushman, K. C., Castillo Butters, L. J., Rojas Vega, C., Roberts, C. B., Kepler, C., & Kellner, J. (2020). Lasers without lost cities: Using drone lidar to capture architectural complexity at Kuelap, Amazonas, Peru. *Journal of Field Archaeology*, 45, S75–S88. <https://doi.org/10.1080/00934690.2020.1713287>
- Yokoyama, R., Shirasawa, M., & Pike, R. J. (2002). Visualizing topography by openness: A new application of image processing to digital elevation models. *Photogrammetric Engineering and Remote Sensing*, 68, 257–265.
- Zakšek, K., Oštir, K., & Kokalj, Ž. (2011). Sky-view factor as a relief visualization technique. *Remote Sensing*, 3(2), 398–415. <https://doi.org/10.3390/rs3020398>
- Zangrando, A. F. (2018). Shell middens and coastal archaeology in southern South America. In C. Smith (Ed.), *Encyclopedia of global archaeology* (pp. 1–15). Springer Nature. [https://doi.org/10.1007/978-3-319-51726-1\\_3024-1](https://doi.org/10.1007/978-3-319-51726-1_3024-1)
- Zangrando, A. F., Borrazo, K., Tivoli, A., Alunni, D., & Martionoli, M. P. (2014). El sitio Heshkaia 35: Nuevos datos sobre la arqueología de Moat (Tierra del Fuego, Argentina). *Revista del Museo de Antropología*, 7, 11–24. <https://doi.org/10.31048/1852.4826.v7.n1.9090>
- Zangrando, A. F. J., Ponce, J. F., Martinoli, M. P., Montes, A., Piana, E. L., & Vanella, F. (2016). Palaeogeographic changes drove prehistoric fishing practices in the Cambaceres Bay (Tierra del Fuego, Argentina) during the middle and late Holocene. *Environmental Archaeology*, 21(2), 182–192. <https://doi.org/10.1080/14614103.2015.1130888>
- Zhou, W., Chen, F., Guo, H., Hu, M., Li, Q., Tang, P., Zheng, W., Liu, J., Luo, R., Yan, K., Li, R., Shi, P., & Nie, S. (2020). UAV laser scanning technology: A potential cost-effective tool for micro-topography detection over wooded areas for archaeological prospection. *International Journal of Digital Earth*, 13(11), 1279–1301. <https://doi.org/10.1080/17538947.2019.1711209>
- Żurkiewicz, D. (2022). Colonists and natives: The beginning of the Eneolithic in the Middle Warta catchment, 4500–3500 BC. *Open Archaeology*, 8(1), 390–401. <https://doi.org/10.1515/opar-2022-0240>

**How to cite this article:** Risbøl, O., Eidshaug, J. S. P., Bjerck, H. B., Gran, M. M., Rantala, K. R., Tivoli, A. M., & Zangrando, A. F. J. (2023). UAV LiDAR in coastal environments: Archaeological case studies from Tierra del Fuego, Argentina, and Vega, Norway. *Archaeological Prospection*, 1–25. <https://doi.org/10.1002/arp.1918>